Image Registration With Fourier-Based Image Correlation: A Comprehensive Review of Developments and Applications

Xiaohua Tong, *Senior Member, IEEE*, Zhen Ye, Yusheng Xu, *Member, IEEE*, Sa Gao, Huan Xie, *Member, IEEE*, Qian Du, *Fellow, IEEE*, Shijie Liu, Xiong Xu, *Member, IEEE*, Sicong Liu, *Member, IEEE*, Kuifeng Luan, and Uwe Stilla, *Senior Member, IEEE*

***Abstract*—Fourier-based image correlation is a powerful area-based image registration technique, which involves aligning images based on a translation model or similarity model by means of the image information and operation in the frequency domain. In recent years, Fourier-based image correlation has made significant progress and attracted extensive research interest in a variety of applications, especially in the field of photogrammetry and remote sensing, leading to the development of a number of subpixel methods that have improved the accuracy and robustness. However, to date, a detailed review of the literature related to Fourier-based image correlation is still lacking. In this review, we aim at providing a comprehensive overview of the fundamentals, developments, and applications of image registration with Fourier-based image correlation methods. Specifically, this review introduces the principal laws underlying these methods, presents a survey of the existing subpixel methods calculated both in the spatial domain and in the frequency domain, summarizes the major applications from three aspects, and discusses the challenges and possible directions of future research. This review is expected to be beneficial for researchers working in the relevant fields to obtain an insight into the current state of the art, to develop new variants, to explore potential applications, and to suggest promising future trends of image registration with Fourier-based image correlation.**

***Index Terms*—Fourier-based image correlation, Fourier-Mellin (FM) transform, image registration, phase correlation (PC), photogrammetry and remote sensing, subpixel image matching.**

Manuscript received March 9, 2019; revised June 18, 2019; accepted August 7, 2019. Date of publication September 18, 2019; date of current version November 22, 2019. This work was supported in part by the National Natural Science Foundation of China under Grant 41631178, in part by the National Key Research and Development Project of China under Grant 2018YFB0505400, in part by the National High Resolution Ground Observation System of China under Grant 11-Y20A12-9001-17/18, in part by the Shanghai Science and Technology Innovation Action Plan Program under Grant 18511102100, and in part by the Fundamental Research Funds for the Central Universities. (*Xiaohua Tong and Zhen Ye contributed equally to this work.*) *(Corresponding authors: Xiaohua Tong; Zhen Ye.)*

X. Tong, S. Gao, H. Xie, S. Liu, X. Xu, and S. Liu are with the College of Surveying and Geo-Informatics, Tongji University, Shanghai 200092, China (e-mail: xhtong@tongji.edu.cn; 1410900@tongji.edu.cn; huanxie@tongji.edu.cn; liusjtj@tongji.edu.cn; xvxiong@tongji.edu.cn; sicong.liu@tongji.edu.cn).

Z. Ye is with the College of Surveying and Geo-Informatics, Tongji University, Shanghai 200092, China, and also with the Department of Photogrammetry and Remote Sensing, Technische Universitaet Muenchen, 80333 Munich, Germany (e-mail: yezhen0402@126.com; z.ye@tum.de).

Y. Xu and U. Stilla are with the Department of Photogrammetry and Remote Sensing, Technische Universitaet Muenchen, 80333 Munich, Germany (e-mail: yusheng.xu@tum.de; stilla@tum.de).

Q. Du is with the Department of Electrical and Computer Engineering, Mississippi State University, Starkville, MS 39759 USA (e-mail: du@ece.msstate.edu).

K. Luan is with the College of Marine Sciences and the Shanghai Engineering Research Center of Estuarine and Oceanographic Mapping, Shanghai Ocean University, Shanghai 201306, China (e-mail: lkf0129@163.com).

Color versions of one or more of the figures in this article are available online at http://ieeexplore.ieee.org.

Digital Object Identifier 10.1109/JSTARS.2019.2937690

I. Introduction

IMAGE registration is the process of overlaying images of the same scene, which can be generally divided into two categories: Feature-based methods and area-based methods [1]. The feature-based methods are normally performed in three steps, i.e., feature detection [2], feature description [3], and feature matching [4]. The salient features, including corner, blob, region, edge, line segment, and shape, are initially extracted from images, and matched using similarity measures and spatial relationships calculated from their descriptors or geometric attributes to establish the geometric correspondence between images. The area-based methods directly utilize the intensity information to match areas or regions, which have advantages in precision, distribution, stability, and other aspects. The focus of the area-based methods is the similarity measure, and the commonly used similarity measures include normalized cross correlation (NCC) [5], sum of squared differences [6], mutual information [7], cross-cumulative residual entropy [8], etc. Fourier-based image correlation is a specific type of area-based image registration technique, which involves aligning images based on a translation model or similarity model by means of the image information and operation in the frequency domain.

Image registration with Fourier-based image correlation possesses the merits of high theoretical accuracy, high computational efficiency, and insensitivity to the frequency-dependent noise and intensity contrast. As a result, it has received a lot of attention in the computer vision, photogrammetry, and remote sensing communities. Due to its remarkable advantages, Fourier-based image correlation has been recommended in many review papers and books concerning image registration [1], [9]–[13]. Since the earliest use of the fast Fourier transform (FFT) for image registration and the introduction of the phase correlation (PC) method in the 1970s [14], [15], Fourier-based image correlation has experienced rapid development, and a

large number of new methods and refinements have since been proposed to enhance the accuracy, robustness, and efficiency. In addition, Fourier-based image correlation has played an important role in various applications, and has an extensive range of potential applications, especially in the field of photogrammetry and remote sensing.

However, while much recent effort has focused on improving the performance and implementing the related applications, less attention has been paid to a unified review of these developments and applications. To the best of our knowledge, no thorough review of Fourier-based image correlation has been written to summarize and discuss this developing topic, except for some partial performance evaluations, such as [16] and [17]. Therefore, it is imperative to survey the current literature to provide guidance for future researches on this topic.

In this review, we provide a comprehensive overview of image registration with Fourier-based image correlation methods, introduce the principal laws underlying these methods, present a survey of the existing subpixel methods, summarize the major applications, and discuss the challenges and possible directions of future researches. This review is intended to not only investigate the current state of Fourier-based image correlation, but also serve as a basis and a starting point for future work, while pointing out the corresponding challenges and tendencies. The ultimate result will be beneficial to the subsequent developments and applications of image registration with Fourier-based image correlation.

The rest of this review is organized as follows. In Section II, we make a brief description of the basic principle of Fourier-based image correlation and the extension to rotation-scaling-translation image registration. Section III investigates and reviews the existing subpixel methods in detail. Section IV presents the major applications of Fourier-based image correlation from three aspects. Challenges and future trends are then discussed in Section V. Finally, the conclusions are drawn in Section VI.

II. Background

A. Correlation Form

Fourier-based image correlation methods implement correlation-like registration of two images in the frequency domain by means of FFT. These methods can be generally divided into two main types of correlation forms, i.e., cross correlation in the frequency domain (CCF) and PC [9], [11]. The major difference between these two types lies in whether or not the approximate normalization in the frequency domain is performed by calculating the phase information [18].

1) Cross Correlation in the Frequency Domain: Cross correlation is a basic statistical approach for finding the degree of similarity between two images or templates. From the well-known *correlation theorem* (or *convolution theorem*), the cross correlation can be alternatively achieved in the Fourier domain [11]. The *correlation theorem* states that the Fourier transform (FT) of the correlation of two images is the product of the FT of one image and the complex conjugate of the FT of the other [9]. If we assume that two image functions $f(x,y)$ and $g(x,y)$ that are related by shifts Δx and Δy in the row and column directions are expressed as $g(x,y) = f(x-\Delta x, y-\Delta y)$, then the correlation function of CCF is given by

$$CC = F^{-1}(F(u,v)^{*}G(u,v)) \tag{1}$$

where $F(u,v)$ and $G(u,v)$ are the corresponding FT of $f(x,y)$ and $g(x,y)$, F^{-1} denotes the inverse FT, and * denotes the complex conjugate. The performance of CCF is equivalent to computing the cross correlation in the spatial domain, while the use of the FFT routine avoids the iterative search of the traditional correlation process and enables the rapid computation of correlations. However, CCF does not involve any kind of normalization and thus tends to be sensitive to the intensity variations. In addition, the frequency domain analysis of CCF implies that the phase difference term that contains the translational information is weighted by the magnitudes of the two images. Due to the low-pass property of natural images, the weighting operation often results in a correlation function with broad peaks of large magnitude and an incorrect dominant peak [19]. Therefore, an effective CCF method requires the integration of a certain type of normalization or image representation.

2) Phase Correlation: Although conventional NCC can be extended to a Fourier-based calculation by means of multiple CCF operations [11], it is still somewhat complex and inefficient. A common way of approximating normalization in the Fourier domain is to perform PC [15], which considers only the phase information and is therefore insensitive to image content.

PC is based on the translation property of FT, which states that a shift of two relevant images in the spatial domain is transformed into the frequency domain as phase differences. The correlation function of PC can be computed from the inverse FT of the normalized cross-power spectrum matrix Q, which can be expressed by

$$\begin{aligned} PC = F^{-1}(Q(u,v)) &= F^{-1}\left\{\frac{F(u,v)^{*}G(u,v)}{|F(u,v)^{*}G(u,v)|}\right\} \\ &= F^{-1}\left\{\exp(-i(u\Delta x + v\Delta y))\right\} \end{aligned} \tag{2}$$

where $i = \sqrt{-1}$. There are several advantages of PC over the classical image correlation methods [1], [9], [18], [20].

1) Similar to CCF, the computational efficiency is high with the help of FFT.
2) The property of solely using the phase information decreases the dependency on image intensity and content, and makes the PC invariant to global linear variations in contrast and brightness.
3) The obtained correlation peak is sharper, which enables the peak location to be more accurate and reliable.
4) As the phase differences at every frequency contribute equally, corruptions limited to a small range of frequencies will not alter the dominant phase difference and will not influence the peak location.

The PC is therefore robust to the frequency-dependent noise, large intensity differences, and time-varying illumination disturbances. On the other hand, the frequency-independent white noise, aliasing, and deformations that spread across all frequencies can make the PC estimates inaccurate. In this case, effective

preprocessing operations or robustness measures are needed to handle the influence of these corruptions. In addition, the PC method can be interpreted from the point of view of the matched filtering techniques as symmetric phase-only matched filtering [11], [21], [22].

Further studies into other properties and improvements of the PC method have been presented. For instance, Alliney and Morandi [23] improved the computational efficiency by projecting the images into each direction and matching the projections using one-dimensional (1-D) FT. A shape adaptive transform was developed to tackle the issue of still background in motion estimation [24], [25]. Discrete cosine transform-based PC methods were proposed in [26] and [27] to reduce the computational effort, especially for image and video coding applications. Blur-invariant PC methods were proposed in [28]–[30] for centrally symmetric blurs, *N*-fold rotational symmetric blurs, and *N*-fold dihedral blurs, respectively. Argyriou [31] proposed a novel PC method operated on the hexagonal lattice. Konstantinidis *et al.* [32] integrated the notion of motion magnification in the PC procedure. In [33] and [34], the illumination robustness of PC was investigated through mathematical analysis and image matching experiments. The statistical analysis of the correlation function of PC was performed [35]–[37]. In [38], biological interpretation and analysis of the role of PC in visual information processing, visual illusion, and pattern recognition were provided. For multichannel color images, vector correlation techniques were proposed in [39] and [40], based on hypercomplex (quaternion) FT [41].

B. Pixel-Level Correlation

The integer solution of Fourier-based image correlation can be achieved in a similar way to the classic cross-correlation method. A peak can be determined within the correlation surface after the inverse FT, whose discrete coordinates correspond to the integer-pixel shifts between two images. It is worth noting that, according to the sampling theorem, the maximum measurable range of the physical shifts from image correlation is half of the correlation window, in the case of no zero padding. The cases for which the locations of the correlation peaks are larger than half the correlation window represent shifts in the inverse direction.

Concerning the PC method, it is simpler to locate the peak of the correlation surface since the inverse FT of the normalized cross-power spectrum matrix Q in (2) theoretically corresponds to a Dirac delta function centered at the unknown displacement $(\Delta x, \Delta y)$, in the case of integer-pixel shifts, i.e.,

$$\begin{aligned} \mathrm{PC} &= F^{-1}(Q(u,v)) = F^{-1}\left\{\exp(-i(u\Delta x + v\Delta y))\right\} \\ &= \delta(x - \Delta x, y - \Delta y). \end{aligned} \tag{3}$$

When dealing with discrete images, the Dirac delta function is replaced by a unit impulse function. In the presence of noise, dissimilar parts, or other corruptions, the value of the peak will decrease, but will still be adequately distinct.

Fig. 1 shows an example to demonstrate the advantages of the PC method. Fig. 1(c) and (d) is the correlation surfaces calculated from the PC and classic NCC of two satellite images with displacements along both directions, as shown in Fig. 1(a) and (b), respectively. An obvious peak can be seen from the correlation surface to obtain the displacements between the two images. The PC method provides a much sharper peak at the corresponding point of the displacements and is approximately zero at the other locations. Fig. 1(g) and (h) is the correlation surfaces calculated from the PC and NCC of two displaced satellite images with different spectral bands, as shown in Fig. 1(e) and (f), respectively. The NCC method yields several broad peaks and a main peak, which may become unstable, whereas the PC method still generates a distinct sharp peak, although the value of the peak is slightly decreased.

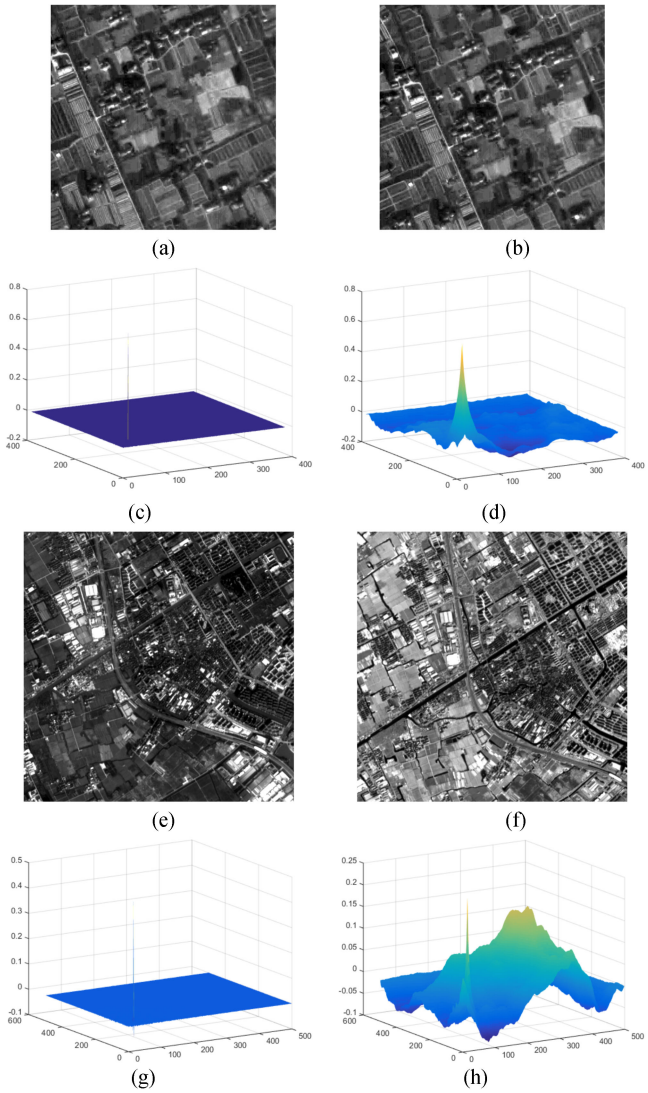

Fig. 1. Example of pixel-level image correlation. (a) and (b) Satellite images with displacements along both directions. (c) and (d) Correlation surfaces calculated from the PC and NCC of the images in (a) and (b), respectively. (e) and (f) Displaced satellite images with different spectral bands. (g) and (h) Correlation surfaces calculated from the PC and NCC of the images in (e) and (f), respectively.

C. Image Registration With Fourier-Mellin (FM) Transform

The above-mentioned introduction mainly focuses on image registration for translation estimation. In order to deal with more

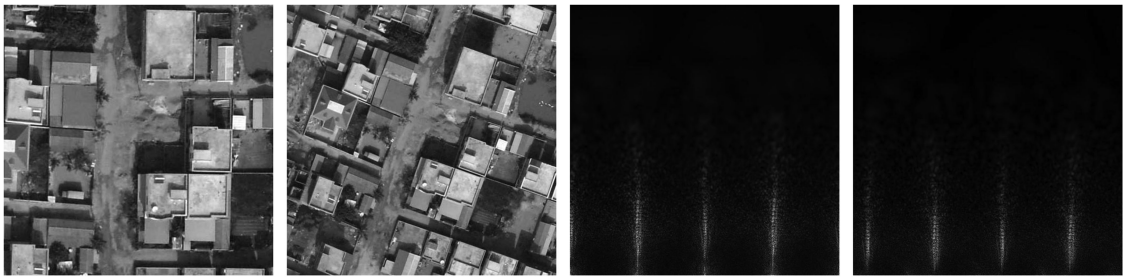

Fig. 2. Example of FM transform. (a) and (b) Two images with rotational, scaling, and translational transformation. (c) and (d) Corresponding FM transforms of (a) and (b), respectively. The rotation angle and scaling factor can be solved from the translational relationship between two log-polar representations.

general image transformation, Fourier-based image correlation has been extended to align images with rotational differences [42], as well as images with both rotational and scaling differences [22], [43]. The extensions rely on the Fourier rotational property and the Fourier scaling property, which is a two-step process to first determine the rotation angle and isotropic scaling factor, and then determine the translational shift. The former method requires the exhaustive search for all possible rotation angles, which is computationally costly. The latter two methods are realized by means of translation-invariant FM transform, which corresponds to the log-polar mapping of the spectral magnitude, achieving a higher computational efficiency in image registration applications [11].

As in the PC method, the translational information of images is encoded only in the phase of FT. Therefore, if the phase information is removed from FT, the scaling and rotational information for images can be retained in the spectral magnitude, without being dependent on the translational information. We consider two image functions $f(x,y)$ and $g(x,y)$ that are related by translation $(\Delta x, \Delta y)$, rotation θ_0, and isotropic scaling s as

$$g(x,y) = f(s(x\cos\theta_0 + y\sin\theta_0) - \Delta x, s(-x\sin\theta_0 + y\cos\theta_0) - \Delta y). \quad (4)$$

According to the shift, rotational, and scaling properties of FT, the corresponding FTs of the two images are related by [22]

$$G(u,v) = s^{-2}F[s^{-1}(u\cos\theta_0 + v\sin\theta_0), s^{-1}(-u\sin\theta_0 + v\cos\theta_0)]\exp[-i\phi_g(u,v)] \quad (5)$$

where $\phi_g(u,v)$ is the spectral phase of $g(x,y)$. Taking the magnitude in both parts of (5) can separate the translational information:

$$M_G(u,v) = s^{-2}M_F[s^{-1}(u\cos\theta_0 + v\sin\theta_0), s^{-1}(-u\sin\theta_0 + v\cos\theta_0)] \quad (6)$$

where M_G and M_F are the magnitudes of *G* and *F*. Applying the log-polar mapping of the magnitudes (i.e., FM transform) can represent the rotation and scaling estimation as translation estimation in an equivalent coordinate system:

$$M_{\mathrm{Glp}}(\lambda,\theta) = s^{-2}M_{\mathrm{Flp}}(\lambda - \log s, \theta - \theta_0) \quad (7)$$

where M_{Glp} and M_{Flp} are the log-polar representations of M_G and M_F. Therefore, the rotation angle and isotropic scaling factor can be estimated using the Fourier-based image correlation method introduced above. After compensating for the rotation and scaling, the translation can be subsequently determined by again implementing a Fourier-based image correlation method. See Fig. 2 for an example of FM transform.

Image registration with FM transform decouples the rotation, scaling, and translation, and can be applied in the case of large motions, without prior knowledge. Further analysis and refinements of this kind of image registration methods have been reported. Stone *et al.* [44] investigated the factors that degrade the precision of image registration based on Fourier-based correlation and demonstrated constructive techniques for reducing the rotationally dependent aliasing, such as cutting off low frequencies, as well as windowing the image to remove the high frequencies. Reddy and Chatterji [43] handled this issue by using a simple high-pass emphasis filter. In addition, the conventional calculation methods of polar/log-polar FTs can be conducted using either image domain warping and then two-dimensional (2-D) FT calculation, or interpolation of the 2-D discrete FT in the Fourier domain [45]. Larger interpolation errors for the low-frequency components are induced by Cartesian-to-log-polar conversion in the FM transform, as log-polar representation is extremely dense in the low frequency [19]. In order to evaluate the polar/log-polar FT efficiently and accurately and reduce the interpolation errors, new sampling schemes and algorithms have been proposed in recent years, including pseudo-polar FT [45], pseudo-log-polar FT [46], polar FT [47], multilayer fractional FT [48], multilayer pseudo-polar fractional FT [49], exact polar FT [50], multilayer polar FT [51], and so on. Keller *et al.* [52] proposed the angular difference function to estimate the rotation angle using pseudo-polar FT without any interpolation step. Tzimiropoulos *et al.* [19] circumvented the problems related to the interpolation errors, edge effects, and aliasing, by alternatively using gradient-based correlation schemes, which can realize Fourier-based image registration with large scaling differences and with higher computational efficiency. Fujisawa and Ikehara [53] applied Radon transform to the frequency domain and the spatial domain of images for rotation and scale estimation. Furthermore, the PC method has been applied to recover the translational component after compensation for the affine matrix in the frequency domain methods for affine transformation estimation [54], [55]. Extensions to 3-D frequency domain volume registration based on Fourier-based image correlation and FM transform have been presented [56]–[61].

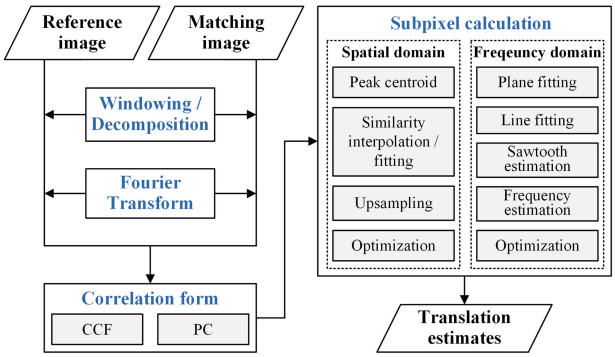

Fig. 3. Overall workflow of subpixel Fourier-based image correlation methods.

III. Subpixel Methods

Foroosh *et al.* [20] derived the analytical expressions for the PC assuming that images with subpixel shifts were originally displaced by integer values on a high-resolution grid, followed by downsampling. In the case of subpixel shifts, the signal power in the PC is not concentrated in a single peak, but rather in several coherent peaks, with the most eminent ones largely adjacent to each other, which implies that PC leads to a downsampled 2-D Dirichlet kernel. Therefore, further processing is required for subpixel Fourier-based image correlation methods. A wide variety of subpixel methods have been proposed over the years, with the advances on different aspects. In this section, we comprehensively investigate and review the existing subpixel Fourier-based image correlation methods presented in the literature.

The subpixel Fourier-based image correlation methods are generally classified into two categories, which can be implemented either in the spatial domain by means of the sharp correlation peak or in the frequency domain by means of the phase differences. In general, in order to reduce the influence of edge effects due to the periodicity assumption of discrete FT, the windowing functions [62] or an image decomposition [63] are used to the input images prior to the image correlation. Fig. 3 shows the overall workflow of subpixel Fourier-based image correlation methods.

A summary of various subpixel Fourier-based image correlation methods according to two subpixel calculation categories is given in Table I. The subpixel calculation methods in the spatial domain include peak centroid, similarity interpolation/fitting, upsampling, and nonlinear optimization, while the subpixel calculation methods directly in the frequency domain include plane fitting, line fitting, sawtooth signal estimation, frequency estimation, and optimization. In the following, the typical alternatives for these two categories of methods are introduced in detail.

A. Subpixel Calculation in the Spatial Domain

Subpixel calculation in the spatial domain is realized by determining the precise subpixel location of the correlation peak after the inverse FT though interpolation, fitting, or other approaches with a certain range of neighbors, which is similar to the subpixel methods for traditional image correlation and similarity-based matching. The subpixel shift is estimated by assuming that the correlation function is continuous and the 2-D correlation surface or 1-D correlation curve approximately conforms to a certain function, or by interpolating the image intensity or the cross-power spectrum to a desired subpixel resolution.

When the shift between two images is noninteger, the energy of the correlation peak spreads across the adjacent pixels. Therefore, an intuitive and straightforward way of subpixel calculation in the spatial domain is by applying the peak centroid, which simply calculates the centroid (or weighted average) of a local neighborhood around the integer-valued peak location. The centroid estimation is based on the fact that the centroid of a symmetric object is equal to the position of the object. However, this is true only on the integer-pixel and half-pixel positions for the discrete correlation, which causes the estimations to be strongly biased toward integer values [64]. For Fourier-based image correlation, the peak centroid method was utilized in [65]–[67] to estimate the subpixel displacement.

Concerning the similarity interpolation/fitting methods, the challenge is that it is usually hard to find a reasonable model that can perfectly describe the discrete correlation surface, especially in the case of real applications. According to the fact that the correlation surface around its peak often approaches a bell shape, a number of models have been tested in empirical and theoretical researches, particular in particle image velocimetry and digital image correlation [68], [69]. The adopted peak fitting models for subpixel Fourier-based image correlation include the quadratic function, the Gaussian function, the Dirichlet function, the sinc function, the modified sinc function, and the modified Mexican hat wavelet (MHW).

The most commonly used fitting model is the quadratic function, namely 1-D parabola fitting and 2-D paraboloid fitting. Applying a quadratic model is theoretically justified only for correlation based on the sum of squared differences. However, it is still used as an approximation in many methods [18], [70]–[72] to estimate the subpixel shifts, due to its closed formula and simple implementation. If we denote a parabolic function as $\tilde{c}(x) = a_0x^2 + a_1x + a_2$, then the subpixel peak location Δx is directly determined using the integer-valued main peak x_0 and its two nearest neighbors as

$$\Delta x = x_0 + \frac{c_{-1} - c_{+1}}{2(c_{-1} - 2c_0 + c_{+1})} \tag{8}$$

where $c_0 = c(x_0), c_{-1} = c(x_0 - 1), c_{+1} = c(x_0 + 1)$, and c denotes the 1-D variable-separable discrete correlation curve, vertically as well as horizontally. If we denote a paraboloid function as $\tilde{C}(x, y) = a_0x^2 + a_1y^2 + a_2xy + a_3x + a_4y + a_5$, then the subpixel peak location $(\Delta x, \Delta y)$ can be obtained based on six coefficients $a_i (i = 0, \ldots, 5)$ as

$$\Delta x = \frac{a_2a_4 - 2a_1a_3}{4a_0a_1 - a_2^2}$$
$$\Delta y = \frac{a_2a_3 - 2a_0a_4}{4a_0a_1 - a_2^2} \tag{9}$$

where the coefficients can be computed using the integer-valued peak (x_0, y_0) and its five selected nearest neighbors, or using least-squares fitting given a larger size of neighbors centered at (x_0, y_0) [16].

TABLE I
SUMMARY OF VARIOUS SUBPIXEL FOURIER-BASED IMAGE CORRELATION METHODS ACCORDING TO TWO SUBPIXEL CALCULATION CATEGORIES

Subpixel category	Solutions and models		Methods and References
Spatial domain	Peak centroid		Michel and Rignot [65], Druckmüller [66], Caron *et al.* [67]
	Similarity interpolation / fitting	Quadratic function	Tian and Huhns [70], Abdou [71], Argyriou and Vlachos [72], Heid and Kääb [18]
		Gaussian function	Abdou [71], Eckstein *et al.* [73], Ren *et al.* [74], Li *et al.* [75], Lynch and Devaney [76]
		sinc derivation	Foroosh *et al.* [20], Nagashima *et al.* [77], Chen and Yap [78], Ren *et al.* [79], Ma *et al.* [80]
		Dirichlet function	Takita *et al.* [81], Takita *et al.* [82], Chen *et al.* [83]
		Modified sinc function	Argyriou and Vlachos [84], Wang and Yan [85]
		Modified Mexican hat wavelet	Tzimiropoulos *et al.* [86], Argyriou and Tzimiropoulos [87], Ye *et al.* [88]
	Upsampling	Zero-padding	Young and Driggers [89], Zhang *et al.* [90], Alba *et al.* [16]
		Matrix multiplication	Guizar-Sicairos *et al.* [91], Wang *et al.* [92], Yousef *et al.* [93]
	Optimization		Roesgen [94], Guizar-Sicairos *et al.* [91], Alba *et al.* [16]
Frequency domain	Plane fitting		Stone *et al.* [95], Malcolm *et al.* [96], Averbuch and Keller [97], Vandewalle *et al.* [98], Liu and Yan [99], González *et al.* [100], Morgan *et al.* [101], He *et al.* [102], Tong *et al.* [103], HajiRassouliha *et al.* [62], Ye *et al.* [104]
	Line fitting		Hoge [105], Foroosh and Balci [106], Hoge and Westin [107], Keller and Averbuch [108], San José Estépar *et al.* [109], Tong *et al.* [110], Wang *et al.* [111] , Chen *et al.* [112], Dong *et al.* [113], Ye *et al.* [88]
	Sawtooth signal estimation		Balci and Foroosh [114], Balci and Foroosh [115], Zuo *et al.* [116]
	Frequency estimation		Xu and Varshney [117]
	Optimization		Kim and Su [118], Abdou [71], Van Puymbroeck *et al.* [119], Leprince *et al.* [120]

The Gaussian function is also popular for fitting the correlation surface. By assuming that the two dimensions are separable and orthogonal, some methods [71], [73]–[76] adopt a 1-D Gaussian function to fit the subpixel peak. The 1-D Gaussian function is defined as

$$\tilde{c}(x) = a_0 \exp\left\{\frac{-(x-a_1)^2}{a_2^2}\right\} \tag{10}$$

where a_0 and a_2 are the parameters that control the height and width of the Gaussian function, and a_1 is the center position of the peak. Using the integer-valued peak x_0 and its two nearest neighbors, the subpixel peak location Δx is given by

$$\Delta x = a_1 = \frac{2x_0(T+1)+(T+1)}{2(T-1)}$$
$$T = \frac{\ln(c_{-1})-\ln(c_0)}{\ln(c_0)-\ln(c_{+1})}. \tag{11}$$

As mentioned above, Foroosh *et al.* [20] derived analytical expressions for the cross-power spectrum of downsampled images and showed that PC yields a 2-D Dirichlet kernel after the inverse FT:

$$C(x,y) = \frac{1}{WH}\frac{\sin(\pi(Mx-x_p))}{\sin(\pi(Mx-x_p)/W)}\frac{\sin(\pi(Ny-y_p))}{\sin(\pi(Ny-y_p)/H)} \tag{12}$$

where x_p and y_p denote the integer shifts before downsampling, *W* and *H* are the image width and height before downsampling, and *M* and *N* are the downsampling scales. The Dirichlet function in (12) can be approximated by a sinc function as

$$\tilde{C}(x,y) \simeq \frac{\sin(\pi(Mx-x_p))}{\pi(Mx-x_p)}\frac{\sin(\pi(Ny-y_p))}{\pi(Ny-y_p)}. \tag{13}$$

Accordingly, using the integer-valued main peak (x_0, y_0) and one concentrated side peak in each direction (x_s, y_0) and (x_0, y_s), where $x_s = x_0 \pm 1$ and $y_s = y_0 \pm 1$, a closed-form solution for the subpixel shifts $(\Delta x, \Delta y)$ can be provided as

$$\Delta x = \frac{x_p}{M} = \frac{\pm R_x x_0 - x_s}{\pm R_x - 1}, \quad R_x = \frac{C(x_0,y_0)}{C(x_s,y_0)}$$
$$\Delta y = \frac{y_p}{N} = \frac{\pm R_y y_0 - y_s}{\pm R_y - 1}, \quad R_x = \frac{C(x_0,y_0)}{C(x_0,y_s)}. \tag{14}$$

There are two solutions in each direction obtained from the above equation, and the correct solution meets the condition that $\Delta x - x_0$ or $\Delta y - y_0$ is in the interval $[-1, 1]$ and has the same sign as $x_s - x_0$ or $y_s - y_0$.

Ren *et al.* [79] indicated that Foroosh's method insufficiently takes into account the interference term, and using only one-sided information is sensitive to noise. Therefore, a refinement that integrates the differences between the two-sided neighbors has been proposed as

$$\Delta x = \frac{\mathrm{sgn}(D_x)}{1 + C(0,0)/|D_x|}, \quad D_x = C(1,0) - C(-1,0)$$
$$\Delta y = \frac{\mathrm{sgn}(D_y)}{1 + C(0,0)/|D_y|}, \quad D_y = C(0,1) - C(0,-1) \quad (15)$$

where sgn denotes the sign function, and $C(0,0)$, $C(1,0)$, $C(-1,0)$, $C(0,1)$, and $C(0,-1)$ are the correlation values at the main peak and side peaks. In addition, higher-order statistics and a higher-order Taylor expansion for approximating the sinc function were employed to enhance the performance under noisy conditions [78].

Differing from the analytical derivations of Foroosh's method, some methods [81]–[83] obtain the subpixel shifts by straightforward fitting of the 2-D Dirichlet function:

$$C(x,y) \simeq \frac{\alpha}{WH} \frac{\sin(\pi(x-\Delta x))}{\sin(\pi(x-\Delta x)/W)} \frac{\sin(\pi(y-\Delta y))}{\sin(\pi(y-\Delta y)/H)} \quad (16)$$

where $\alpha \leq 1$ denotes the correlation peak value, which implies the matching reliability, and Δx and Δy represent the subpixel peak location. The parameters $(\alpha, \Delta x, \Delta y)$ can be solved by nonlinear regression with a set of points including the integer-valued main peak and its neighbors.

On the basis of Foroosh's method [20] and Takita's method [81], a so-called peak evaluation formula (PEF) derived from the 1-D sinc function fitting was introduced in [77], through which the subpixel shifts can be achieved from multiple tri-tuples consisting of the main peak and its corresponding surrounding points. After approximating (16) to a sinc function and separating it into a 1-D case, the correlation peak model is given by

$$c(x) = \beta \frac{\sin(\pi(x-\Delta x))}{\pi(x-\Delta x)}. \quad (17)$$

Therefore, the correlation values of a tri-tuple $(p-d, p, p+d)$ satisfy the following formula:

$$(p-d-\Delta x)\cdot c(p-d) + (p+d-\Delta x)\cdot c(p+d) = 2(p-\Delta x)\cdot \cos(\pi d)\cdot c(p) \quad (18)$$

where p denotes the reference point, and d denotes the distance. The equation given above can be rewritten as

$$\begin{aligned} v(p,d) &= u(p,d)\cdot \Delta x \\ u(p,d) &= c(p-d) + c(p+d) - 2\cos(\pi d)\cdot c(p) \\ v(p,d) &= (p-d)\cdot c(p-d) + (p+d)\cdot c(p+d) \\ &\quad - 2p\cdot \cos(\pi d)\cdot c(p). \end{aligned} \quad (19)$$

By selecting different reference points p and distances d, multiple tri-tuples can be generated to estimate the subpixel shifts through the equation given above, without the need of an iterative process.

In [84], a modified esinc function was proposed to fit the exact subpixel peak location, which is defined as

$$\mathrm{esinc}(x) = \exp(-x^2)\frac{\sin\pi x}{\pi x}. \quad (20)$$

The esinc function utilizes Gaussian weighting of a conventional sinc function, which can better approximate the noisy correlation surface. Considering the magnitude, scale, and shift changes, the 1-D correlation curve is represented in the form of $a_0\mathrm{esinc}(a_1(x-a_2))$ as

$$c(x) = a_0\exp(-(a_1(x-a_2))^2)\frac{\sin\pi(x-a_2)}{\pi(x-a_2)}. \quad (21)$$

The unknown parameters (a_0, a_1, a_2) can be calculated by least squares fitting using the correlation values of the main peak and its nearest neighbor on each side, where parameter a_2 corresponds to the subpixel peak location.

Another modified 1-D sinc function, namely the msinc function, was created considering the influence of noise [85]. The correlation curve is approximated by the msinc function as

$$c(x) = a_0\frac{\sin\pi(x-a_1)}{\pi(x-a_1)} + a_2. \quad (22)$$

Similarly, the unknown parameters (a_0, a_1, a_2) can be obtained using the correlation values of the main peak and its neighbors, where parameter a_1 corresponds to the subpixel peak location.

In [86], through analyzing the structure of the correlation function, a modification of the MHW was adopted as a 1-D fitting kernel to provide accurate estimates of the subpixel shifts, which is given by

$$c(x) = a_0\{1-(a_1(x-\Delta x))^2\}\frac{1}{\sqrt{2\pi}a_2}\exp\left(\frac{-(x-\Delta x)^2}{2a_2^2}\right). \quad (23)$$

The kernel parameter $(\Delta x, a_0, a_1, a_2)$ can be numerically solved in a nonlinear least-squares sense using a set of correlation samples.

Besides similarity interpolation/fitting, Fourier-based image correlation can also perform subpixel calculation via intensity interpolation, in a similar way to the conventional area based image matching methods, which interpolate the image to a desired resolution prior to image correlation [69]. However, this approach is too computationally expensive, especially for large-scale applications. With regard to Fourier-based image correlation, we can alternatively realize a computationally efficient implementation of subpixel shift estimation by upsampling the computed cross-power spectrum, since the correlation of two upsampled images is equivalent to upsampling the correlation of two original images [89], [121]. In order to reduce the computational burden and memory requirement, a local upsampling strategy should be performed, which oversamples

the cross-power spectrum in a tiny neighborhood around the initial peak location estimate.

Upsampling the cross-power spectrum in the frequency domain can be implemented by either zero padding or matrix-multiply discrete FT. It is noted that zero padding the frequency signal is equivalent to interpolating the corresponding time signal. In [16], [89], and [90], zero padding was used to acquire an upsampled correlation for subpixel estimation. On the other hand, using an implementation based on matrix-multiply discrete FT can achieve similar performance to zero padding, and is more suitable for local upsampling with lower computational complexity. Therefore, a number of methods [91]–[93] have adopted matrix multiplication-based upsampling to interpolate the local discrete correlation surface. In addition, an iterative search scheme can be applied to further improve the computational efficiency, which gradually reduces the neighborhood size and upsampling factor to refine the new estimate [91].

Another feasible alternative for subpixel calculation in the spatial domain is the direct search for the real peak location of the correlation function through nonlinear optimization [16], [91], [94]. The correlation function, which is defined as the inverse FT of the cross-power spectrum, can be expressed by

$$C(x,y)=\sum_{u=0}^{W-1}\sum_{v=0}^{H-1}Q(u,v)\exp\left\{i2\pi\left(\frac{ux}{W}+\frac{vy}{H}\right)\right\}. \quad (24)$$

In order to find the extrema of $C(x,y)$, its derivative is given by

$$\begin{aligned}\nabla C(x,y)&=\left[\frac{\partial C}{\partial x}(x,y),\frac{\partial C}{\partial y}(x,y)\right]\\ \frac{\partial C}{\partial x}(x,y)&=-\frac{2\pi}{W}\sum_{u=0}^{W-1}\sum_{v=0}^{H-1}u\mathrm{Im}\\ &\quad\times\left\{Q(u,v)\exp\left\{i2\pi\left(\frac{ux}{W}+\frac{vy}{H}\right)\right\}\right\}\\ \frac{\partial C}{\partial y}(x,y)&=-\frac{2\pi}{H}\sum_{u=0}^{W-1}\sum_{v=0}^{H-1}v\mathrm{Im}\\ &\quad\times\left\{Q(u,v)\exp\left\{i2\pi\left(\frac{ux}{W}+\frac{vy}{H}\right)\right\}\right\}\end{aligned} \quad (25)$$

where Im denotes the operator that takes the imaginary part. The subpixel peak location can be solved by finding the zeros of $\nabla C(x,y)$. Alternatively, we can approximate it by minimizing the real-valued magnitude of the gradient [16]. This sets up the following nonlinear optimization problem:

$$(\Delta x,\Delta y)=\mathrm{argmin}\|\nabla C(x,y)\|^2. \quad (26)$$

An appropriate starting point for the optimization is provided by the integer-valued peak location. It has been suggested that applying the Nelder–Mead method to solve the problem is better as it avoids the computation of the second-order derivative of $C(x,y)$ that has an increased high-frequency content [16].

B. Subpixel Calculation in the Frequency Domain

Subpixel calculation in the frequency domain is free of the inverse FT process, and it explicitly finds the best approximation to the phase difference between two images considering the translation property of FT.

In continuous cases, according to the analytical expression of the normalized cross-power spectrum in (2) associated with Euler's formula, the phase difference, which is defined as the phase angle of the cross-power spectrum, is given by

$$\varphi(u,v)=\angle Q(u,v)=-(u\Delta x+v\Delta y) \quad (27)$$

which represents a 2-D plane defined by the shift parameters through the origin of the *u*-*v* coordinates. As a result, the subpixel shifts Δx and Δy can be computed as the slopes along the two frequency axes by finding the best plane fitting of the phase difference [95], [96], [98].

If the interference term is ignored, the normalized cross-power spectrum matrix is theoretically a rank-one matrix, since each element $Q(u,v)$ is separable, such that

$$\begin{aligned}Q(u,v)&=\exp(-i(u\Delta x+v\Delta y))\\ &=\exp(-iu\Delta x)\exp(-iv\Delta y)=q_x(u)q_y(v).\end{aligned} \quad (28)$$

This implies that the problem of determining the subpixel shifts can be simplified by finding the optimum rank-one approximation of the normalized cross-power spectrum matrix. In [105], the best low-rank approximation was achieved by the singular value decomposition (SVD) method according to the Eckart–Young–Mirsky theorem. The subpixel shifts in two directions can be subsequently recovered by independent line fitting of the phase angle of the left and right domain singular vectors. High-order SVD can be adopted for multidimensional datasets [107], [109]. In [112] and [113], the low-rank matrix factorization with a mixture of Gaussian model and maximum principal component analysis was, respectively, utilized to consider more complicated noise and computational efficiency. Alternatively, it was found that the subspace approximation is not really required, and the subpixel shifts can be estimated by directly fitting the rows and columns of the phase difference matrix [106]. However, the Eigen-filtering nature of SVD makes the estimation less sensitive to noise.

In discrete cases, the phase difference is 2π wrapped in two dimensions in practice. As a result, 2-D phase unwrapping is required before the plane fitting process, and 1-D phase unwrapping is required before the line fitting process, when determining shifts of higher than half a pixel. It is worth noting that 2-D phase unwrapping is a notoriously ill-posed and time-consuming problem. Fortunately, the unwrapping of a 2-D phase difference matrix has been found to be separable, and it can be performed by two independent and consecutive 1-D unwrappings along two directions [106]. Moreover, weighted phase unwrapping can be employed to reduce the influence of noise [111]. It was stated in [100] that phase unwrapping is not a mandatory step when using robust model estimation. However, the addition of the unwrapping process can generate more effective and stable estimates, especially in the case of noisy conditions and larger displacements.

The discrete phase difference matrix has been demonstrated to be a 2-D periodic sawtooth signal [114], [115]. Note that the numbers of repeated cycles along each row and each column of the phase difference matrix correspond to the shift parameters. For this reason, the subpixel shifts can be estimated by finding how many cycles of the sawtooth phase difference fit in the range $[0, 2\pi]$ along each frequency axis, without the need for the unwrapping process. This problem can be solved by a constrained least squares estimation, either using a set of zero crossings of the phase difference matrix and Hough transform [115], or by imposing a rank constraint for the phase difference and a shape constraint for the gradient filter [114]. In [116], the phase of the cross-power spectrum difference was calculated, which was shown to be a discrete 2-D periodic binary stripe signal. Similarly, the subpixel shifts can be determined by counting the number of cycles of the phase matrix of the cross-power spectrum difference along each axis, using the phase discontinuities and Hough transform.

In addition, determining the subpixel shifts can be considered as an instantaneous frequency estimation problem of the cross-power spectrum in the frequency domain [119]. For instance, a subspace-based frequency estimation method was applied in [117] for subpixel Fourier-based image correlation, which calculates the subpixel shifts by applying the multiple signal classifier algorithm to the correlation matrix of data along each axis.

Nonlinear optimization is another typical approach for subpixel calculation. In the frequency domain, the objective function can be formulated by means of the measured cross-power spectrum $Q(u, v)$ and the theoretical one $S(u, v) = \exp(-i(u\Delta x + v\Delta y))$. For instance, an optimization-based method was proposed based on the Hermitian inner product [71], [119]. The projection of Q onto the continuous space defined by the theoretical normalized cross-power spectrum is given by

$$P_{Q,S}(\Delta x, \Delta y) = \sum_u \sum_v Q(u, v) S^*(u, v) = \sum_u \sum_v Q(u, v) \exp(i(u\Delta x + v\Delta y)). \quad (29)$$

The subpixel shifts are estimated by maximizing the modulus $|MP_{Q,S}(\Delta x, \Delta y)|$, where M is a binary mask to filter out some corrupted frequencies. In [120], an improved method was provided, which minimizes the Frobenius norm of the difference between the measured and theoretical cross-power spectrum. The cost function is defined as

$$\phi(\Delta x, \Delta y) = \sum_{u=-\pi}^{\pi} \sum_{v=-\pi}^{\pi} W(u, v) \cdot |Q(u, v) - \exp(-i(u\Delta x + v\Delta y))|^2 \quad (30)$$

where W is a certain frequency weighting or masking matrix. It can be verified that minimizing $\phi(\Delta x, \Delta y)$ is equivalent to maximizing the real part of $MP_{Q,S}(\Delta x, \Delta y)$, if using the same mask. The optimization problem can be solved by a gradient descent algorithm with appropriate initialization, e.g., the two-point step size algorithm.

C. Summary

A simulated correlation test with ground truth was carried out to investigate the performance of subpixel Fourier-based image correlation methods. Twenty one synthetic image pairs were generated from bicubic interpolation of a reference image with subpixel shifts ranging from -1 to 1 pixels by a step of 0.1. It is noted that a certain amount of aliasing is introduced in the resampled images since the ideal interpolation is not realized, which leads to correlation biases for different subpixel methods. Subpixel shifts were calculated using correlation windows of 64×64 pixels scanning the images with a constant step of 32 pixels in each direction. Eleven representative subpixel methods, including peak centroid, parabola fitting, Gaussian fitting, 2-D sinc derivation (Foroosh) [20], 1-D sinc derivation (PEF) [77], modified sinc function (esinc) [84], modified MHW [86], upsampling [91], plane fitting [104], line fitting [110],and optimization [120], are compared. Two hundred and ten thousand correlation measures are gathered in total for each method. The performance is assessed by examining the absolute errors between the estimates and the ground truth. The experimental results are shown in Fig. 4 in the form of boxplots with the mean absolute error below the labels.

In summary, the subpixel Fourier-based image correlation methods calculated in the spatial domain is normally more computationally efficient, but less robust, while the subpixel methods calculated in the frequency domain is normally more accurate, but more time consuming. The performance of the subpixel calculation in the spatial domain is highly dependent on the data quality, the interpolation algorithm, and the approximation degree of the fitting model to the actual peak shape. The peak centroid method and simple interpolation methods suffer from the systematic errors and are sensitive to the practical noises. The subpixel resolution and computational time of upsampling method is determined by the upsampling factor. Using the specifically designed fitting models and nonlinear optimization can improve the performance to some extent. In contrast, the subpixel Fourier-based image correlation methods calculated in the frequency domain avoid inverse transforming the cross-power spectrum and directly rely on the mathematical expression of phase difference. Aliasing, noise, and other artifacts, which are mainly located at the high-frequency components in the Fourier domain, become dispersed in the spatial domain [106]. Therefore, avoiding the inverse FT process contributes to dealing with these artifacts, in a theoretical sense. Several additional measures, such as frequency masking [95], [120] and robust estimation [110], [114], can be easily implemented in the workflow to enhance the robustness and accuracy under uncontrolled conditions. But these measures also inevitably cost more computation time. The selection of an appropriate subpixel Fourier based image correlation method in the real applications is driven by implementation detail, matching strategy, image quality and scene condition, as well as requirements in accuracy, robustness, resolution, and efficiency.

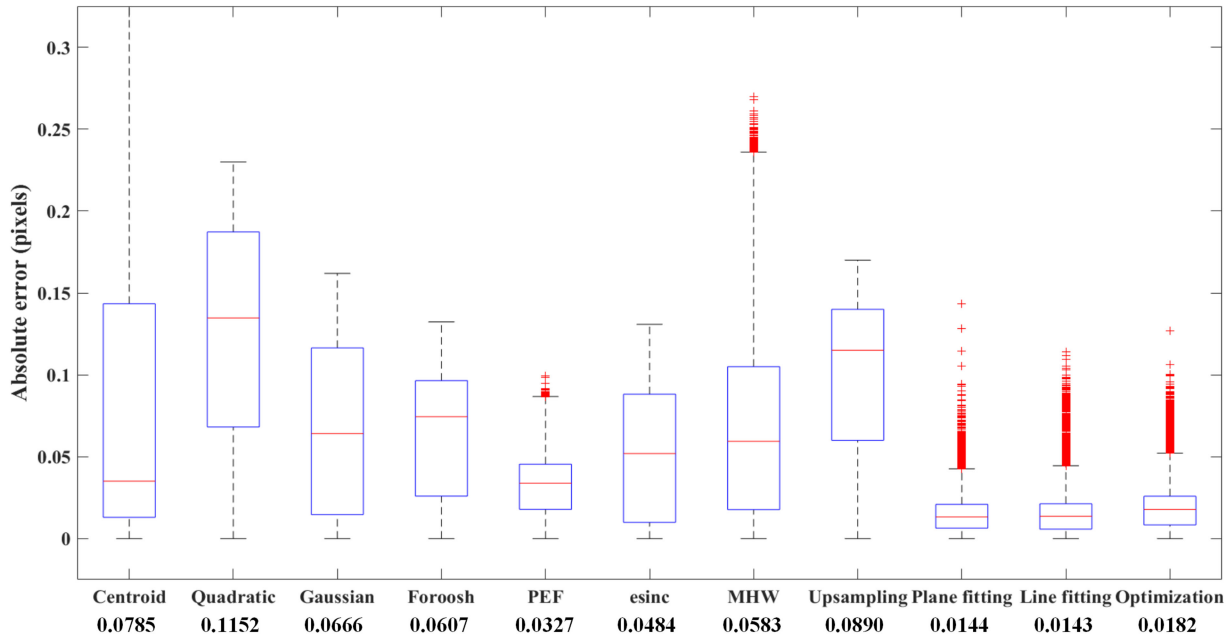

Fig. 4. Boxplots of the absolute errors for different subpixel methods. The mean absolute error of each method is listed below the labels.

IV. Major Applications

Advances in algorithms with better performances have promoted the broader application of Fourier-based image correlation methods. Generally speaking, there are three different ways of utilizing Fourier-based image correlation in applications: 1) evaluation of similarity to provide a good similarity measure between images, which is required in several recognition and classification tasks; 2) global image registration, which involves aligning two corresponding images with a similarity transformation by means of FM transform; and 3) local displacement estimation, which involves calculating accurate shift values between patches at some key points, or in a dense manner. A broad range of applications and extensions can benefit from Fourier-based image correlation methods, especially with higher accuracy, robustness, and computational efficiency. In this review, we present a brief overview of these applications from three aspects: 1) image registration extension; 2) close-range imagery and signals; and 3) remote sensing imagery. Table II shows a nonexhaustive list of the major applications in these three aspects.

A. Image Registration Extension

Image registration with Fourier-based image correlation and FM transform can recover a rotation-scale-translation model between images. The most direct applications are developing hybrid registration frameworks associated with other registration algorithms and aligning specific types of images.

The roles of image registration with Fourier-based image correlation and FM transform in a hybrid registration framework lie in two aspects. On the one hand, global registration with FM transform is free of iteration, and can thus directly work in the presence of large motions. More importantly, its computational cost is independent of the transformation value and scene complexity. Therefore, it can be complementary to other algorithms to realize efficient image registration. For instance, it can provide a suitable initial approximation, and thus facilitate the convergence for the iteration-based registration algorithms, such as the Keren algorithm [122], [123], the inverse-compositional Gauss–Newton algorithm [124], and the Lucas-Kanade algorithm [125], [126]. It can also provide an initial predicted location, and thus decrease the search range for feature-based matching [127], [128]. On the other hand, template matching based on Fourier-based image correlation can achieve accurate and efficient translation estimation, which is conducive to finding the corresponding feature points and can improve the precision of feature-based matching [129].

In addition, as image registration using Fourier-based image correlation and FM transform is robust to radiometric difference and noise, it has been widely adopted to register different types of 2-D or 3-D images, such as medical images [109], [130], solar coronal images [66], sonar images [131], [132], InSAR images [133], hyperspectral images [134], and multisource remote sensing images [99], [135].

B. Close-Range Imagery and Signals

Fourier-based image correlation methods have been commonly used to process close-range imagery and signals for different purposes, due to their compelling advantages on accuracy and efficiency over the traditional spatial correlation methods. In the field of biometric recognition and matching [136], PC and its extensions have been extensively adopted to measure the global similarity between images in various biometric authentication tasks, such as fingerprint matching [137], iris recognition [138], finger knuckle print recognition [139], face recognition

TABLE II
LIST OF APPLICATIONS USING FOURIER-BASED IMAGE CORRELATION

Application aspect	Application description		Examples
Image registration with Fourier-based correlation and FM transform	FM transform & Keren algorithm		Li [122], Zhou *et al.* [123]
	FM transform & inverse-compositional Gauss-Newton algorithm		Pan *et al.* [124]
	FM transform & Lucas-Kanade algorithm		Douini *et al.* [125], Li [126]
	FM transform & feature-based matching		Zhao *et al.* [127], Li *et al.* [128], Li and Man [129]
	InSAR image registration		Abdelfattah and Nicolas [133]
	Hyperspectral image registration		Erives and Fitzgerald [134], Ordóñez *et al.* [194], [195]
	Medical image registration		Wilson and Theriot [130], San José Estépar *et al.* [109], Kolar *et al.* [196], Vaillant *et al.* [197]
	Multi-sensor image coregistration		Liu and Yan [99], Scheffler *et al.* [135], Skakun *et al.* [198], Henke *et al.* [199]
	Solar coronal image registration		Druckmüller [66]
	Sonar image registration		Bülow and Birk [131], Li *et al.* [200], Hurtós *et al.* [132]
Close-range imagery and signals	Biometric recognition and matching		Ito *et al.* [137], Miyazawa *et al.* [138], Zhang *et al.* [139], Rizo-Rodríguez *et al.* [140], Mohd Asaari *et al.* [141], Rida *et al.* [142], Kumar [143]
	Disparity (3D) acquisition		Takita *et al.* [82], Muquit *et al.* [201], Chen *et al.* [83]
	Geophysical processing		Moriya [144], Wu *et al.* [202], Tomar *et al.* [145]
	Image processing and analysis	Auto-focusing	Jang *et al.* [146]
		Digital image stabilization	Ertürk [147], Kumar *et al.* [203]
		Duplication detection	Wu *et al.* [148], Shao *et al.* [204]
		Image watermarking	Zheng *et al.* [149], Kang *et al.* [205], Ouyang *et al.* [206]
		Nonuniformity correction	Zuo *et al.* [150], Liu and Xie [207], Caron *et al.* [67]
		Super-resolution	Vandewalle *et al.* [98], Young and Driggers [89]
		Symmetry detection	Keller and Shkolnisky [151], Tzimiropoulos *et al.* [208]
	Video processing and analysis	Cut detection	Vlachos [152], Urhan *et al.* [209]
		Video alignment	Dai *et al.* [153], Jia *et al.* [210]
		Video coding	Mittal *et al.* [211], Ismail *et al.* [212], Paul *et al.* [154]
		Video quality measurement	Barkowsky *et al.* [155]
	Motion estimation and tracking (others)	Electron backscatter diffraction measurement	Miyamoto *et al.* [156], Riedl and Wendrock [213]
		Laboratory seismic measurement	Caniven *et al.* [214], Rubino *et al.* [157]
		Medical image analysis	Kelly *et al.* [158], de Oliveira *et al.* [215], Krafft *et al.* [216]
		MEMS measurement	Serio *et al.* [217], Teyssieux *et al.* [159]
		Micro/Nano analysis	Yang *et al.* [160], Recknagel and Rothe [218], Cizmar *et al.* [219], Marturi *et al.* [161]
		Particle image velocimetry	Roesgen [94], Thomas *et al.* [162], Eckstein and Vlachos [220], Raben *et al.* [221]

(CONTINUED.) LIST OF APPLICATIONS USING FOURIER-BASED IMAGE CORRELATION

		Structural dynamics measurement	Hild *et al.* [222], Sawada and Sakamoto [223], Feng *et al.* [163], Wang *et al.* [224]
		Visual compass/odometry	Morbidi and Caron [164], Birem *et al.* [225]
		Visual tracking	Zhang *et al.* [165]
Remote sensing imagery	GCP acquisition		Leprince *et al.* [120], Jiang *et al.* [170], Tang *et al.* [226]
	Hyperspectral image processing		Ertürk and Ertürk [167], Demir and Ertürk [168], Çeşmeci and Güllü [169]
	Narrow baseline stereo		Morgan *et al.* [101], Li *et al.* [75], Ma *et al.* [80], Ye *et al.* [227]
	Surface dynamics monitoring	CIAS/OC-Glacier	Dehecq *et al.* [173], Han *et al.* [228], Schaffer *et al.* [229], Sakakibara and Sugiyama [230]
		COSI-Corr-Earthquake	Taylor *et al.* [172], Avouac *et al.* [231], Elliott *et al.* [232], Socquet *et al.* [233]
		COSI-Corr-Glacier	Scherler *et al.* [174], Gantayat *et al.* [234], Armstrong *et al.* [235], Shen *et al.* [236]
		COSI-Corr-Landslide	Lucieer *et al.* [176], Stumpf *et al.* [237], Turner *et al.* [238], Bontemps *et al.* [239]
		COSI-Corr-Sand dune	Necsoiu *et al.* [178], Bridges *et al.* [179], Ayoub *et al.* [240], Michel *et al.* [241]
		COSI-Corr-Others	de Michele *et al.* [180], [181]
		Others	Van Puymbroeck *et al.* [119], González *et al.* [100], Thomas *et al.* [182], Berg and Eriksson [183], Lacroix *et al.* [177], Fang *et al.* [175]
	Misalignment analysis and correction (others)	Attitude jitter detection and analysis	Iwasaki [184], Mumtaz and Palmer [242], Tong *et al.* [185], [243], Ye *et al.* [244]
		Attitude model validation	Pan *et al.* [186]
		Georeferencing improvement	Pardo-Pascual *et al.* [187], Mumtaz *et al.* [188], Almonacid-Caballer *et al.* [245]
		Motion/Change detection	Kääb and Leprince [189], Wan *et al.* [190], Skakun *et al.* [246]
		On-orbit calibration	Leprince *et al.* [191], Yokoya *et al.* [192]
		Orthoimage assessment	Dong *et al.* [193]

[140], finger vein recognition [141], gait recognition [142], and palmprint recognition [143]. In the field of geophysical processing, Fourier-based image correlation has been explored to identify similar microseismic events by evaluating the waveform similarity of time-frequency representations [144] and to measure the subsample vertical and horizontal displacement components in time-lapse seismic [145].

Furthermore, a variety of tasks in image and video processing and analysis benefit from the use of Fourier-based image correlation methods. The exemplary tasks introduced in the literature include auto focusing [146], digital image stabilization [147], duplication detection [148], image watermarking [149], nonuniformity correction [150], super resolution [98], symmetry detection [151], cut detection [152], video alignment [153], video coding [154], and video quality measurement [155]. Besides, some studies have adopted Fourier-based image correlation methods in a dense manner to estimate the disparity between stereo images and implement 3-D measurement [82], [83]. There have also been many studies that have focused on using Fourier-based image correlation methods to achieve motion estimation and tracking in diverse research areas. The prominent application scenarios include electron backscatter diffraction measurement [156]; laboratory seismic measurement [157]; medical image analysis [158]; microelectromechanical system (MEMS) measurement [159]; micro/nano analysis, including drift compensation [160] and nanopositioning [161]; particle image velocimetry [162]; structural dynamics measurement [163]; visual compass [164]; and visual tracking [165].

C. Remote Sensing Imagery

With the development of sensor technology and the growing volume of ground observation data, image registration with Fourier-based image correlation has drawn more and more attention in the remote sensing community. In addition to the global alignment of remote sensing images, Fourier-based image correlation methods can provide precise displacement estimation and reliable similarity evaluation in remote sensing applications. In the field of hyperspectral image processing [166], the peak value of the PC has been successfully used as a similarity measure for different tasks, such as segmentation [167], redundancy removal [168], and classification [169].

Most of the applications in remote sensing rely on dense matching based on Fourier-based image correlation methods in order to obtain detailed information from the remote sensing imagery. The application scenarios include, but are not limited to ground control point (GCP) acquisition, narrow baseline stereo, surface dynamics monitoring, and misalignment analysis and correction. In contrast to the conventional GCP acquisition by field survey, some studies have applied high-accuracy PC methods to efficiently obtain an adequate number of GCPs from reference imagery and topographic data, which is of great importance for the subsequent processing [120], [170]. Compared with the traditional wide baseline stereo configuration, narrow baseline stereo has the advantages of a lower possibility of occlusion, low illumination variation, and more similar viewing geometries, but places a higher demand on the precision of the subpixel image matching. In this case, subpixel Fourier-based image correlation methods, especially PC methods, tend to be a suitable choice and have been applied in several studies of precise disparity estimation from narrow baseline stereo [75], [80], [101]. With the increasing availability of high-quality remote sensing images, a growing number of studies are focusing on the monitoring of surface changes due to geologic processes, climate change, or anthropic activity by comparing pairs of repeat images acquired on different dates [120]. Due to the limited resolution of remote sensing imagery, precise image matching is a core component in such applications and largely determines the final performance. Subpixel Fourier-based image correlation has gradually become a principal tool for ground deformation measurement in recent years. For example, Leprince *et al.* [120] proposed an optimization-based subpixel PC method and developed a complete software package called Co-registration of Optically Sensed Images and Correlation (COSI-Corr), with the objective of retrieving ground surface deformation from multitemporal images. Heid and Kääb [18] explored and evaluated the use of orientation correlation (OC) [171] in applications of glacier surface velocity measurement, and developed free software called Correlation Image Analysis Software (CIAS). On this basis, various subpixel Fourier-based image correlation methods have been successfully adopted to investigate the surface dynamics resulting from diverse natural phenomena not only on Earth, but also on Mars and other planets, such as earthquakes [100], [119], [172], ice flows [173]–[175], landslides [176], [177], sand dune migration [178], [179], ocean waves [180], volcanic eruptions [181], and sea ice [182], [183]. In addition, the high-accuracy misalignments acquired by matching a remote sensing image with a near-simultaneous image or a reference image using subpixel Fourier-based image correlation methods can retrieve a large amount of useful information. All this information reflects not only the quality of the sensor and the geometric processing, but also the motion state of the target and platform. Therefore, subpixel Fourier-based image correlation methods play an important role in a variety of misalignment analysis and correction tasks for different purposes, such as attitude jitter detection and analysis [184], [185], attitude model validation [186], georeferencing improvement [187], [188], motion detection of target [189], and vision-based localization of platform [190], on-orbit calibration [191], [192], and orthoimage assessment [193].

V. Challenges and Future Trends

Although substantial progress has been achieved in Fourier-based image correlation in the past years, there is still room for improvement, and many issues require further investigation. Several challenges and potential future directions are discussed below.

1) *High-accuracy and high-efficiency subpixel methods:* In general, it is a tradeoff problem between accuracy and efficiency. It is therefore encouraging to develop subpixel methods with high performance in practical challenges, and to reduce the computational cost of the best-performing methods. This will significantly facilitate the remote sensing applications with large-scale and high-resolution imagery.
2) *Handling the issue of small window size:* Following Heisenberg's uncertainty principle, Fourier-based image correlation methods are hypothesized to perform worse than the spatial domain correlation methods on small window sizes [18]. This issue has also been found in practical applications [247]. A possible way to address this issue is using a suitable image representation considering overlapping neighboring information [87]. Further study into improving the performance in the case of small window sizes is highly recommended. With the small window size for dense matching and motion estimation, more details can be preserved by Fourier-based image correlation, and the result resolution can be increased.
3) *Effective task-oriented matching frameworks for different applications:* The rapid expansion of image data and the remarkable progress of the subpixel methods offer more potential applications to Fourier-based image correlation. However, different tasks and scenarios have different requirements. In addition to the methods, further improvements should also concentrate on developing advanced task-oriented matching frameworks, including algorithm implementation, hierarchical and adaptive matching strategies, as well as intelligent preprocessing and postprocessing procedures. Several matching frameworks have already been proposed in some previous works, such as [75], [82], [83], and [248]. In order to ensure satisfactory performance, specific matching frameworks for diverse applications in photogrammetry, remote sensing, and other fields should be further designed.
4) *Quantitative comparison in algorithms, implementations, and processing frameworks:* It is worth carrying out the performance evaluation with public benchmark datasets for diverse applications, such as alignment, motion monitoring, disparity estimation, and similarity measurement. The comparative analysis provides more possibilities to boost the performance and robustness of Fourier-based image correlation in real cases, and to explore the systematic error characteristics, e.g., interpolation artifacts

and pixel locking effects [110]. On the other hand, this would also contribute to the selection of optimal algorithms, implementations and processing frameworks in different applications as well as offer opportunities for new applications [189].

VI. Conclusion

Image registration with Fourier-based image correlation has become a vital tool in various research fields and has been broadly used in many different applications due to its compelling advantages and promising capabilities. In recent years, it has attracted considerable attention and made significant progress, especially for subpixel methods. Therefore, in this review, we have extensively summarized and investigated most of the essential works in the literature related to the existing Fourier-based image correlation methods and applications. This gathered analysis will allow us to obtain an insight into the current state of the art, to develop new variants, to explore potential applications, and to suggest promising future trends.

The basic principles underlying Fourier-based image correlation methods and the extension to rotation-scaling-translation image registration with FM transform have been introduced. To provide a common context for the various subpixel methods, the state-of-the-art subpixel Fourier-based image correlation methods have been surveyed according to two categories, i.e., subpixel calculation in the spatial domain and in the frequency domain. The typical solutions and models in each category have been outlined and discussed. In addition, the recent advances of Fourier-based image correlation methods have greatly promoted a wide variety of applications. We have briefly reviewed the major applications from three aspects: Image registration extension, close-range imagery and signals, and remote sensing imagery.

Several challenges and emerging trends for improving the performance and efficiency in the applications have been discussed. It is expected that future developments and applications of image registration with Fourier-based image correlation will continue to be put forward in the upcoming years.

Acknowledgment

The authors would like to thank the editors and the anonymous reviewers for their valuable comments on the improvement of this article.

References

[1] B. Zitova and J. Flusser, "Image registration methods: A survey," *Image Vis. Comput.*, vol. 21, no. 11, pp. 977–1000, 2003.

[2] T. Tuytelaars and K. Mikolajczyk, "Local invariant feature detectors: A survey," *Found. Trends. Comput. Graph. Vis.*, vol. 3, no. 3, pp. 177–280, 2008.

[3] K. Mikolajczyk and C. Schmid, "A performance evaluation of local descriptors," *IEEE Trans. Pattern Anal. Mach. Intell.*, vol. 27, no. 10, pp. 1615–1630, Oct. 2005.

[4] A. Gruen, "Development and status of image matching in photogrammetry," *Photogramm. Rec.*, vol. 27, no. 137, pp. 36–57, 2012.

[5] J. P. Lewis, "Fast template matching," in *Proc. Vis. Interface*, Quebec City, QC, Canada, 1995, pp. 120–123.

[6] J. Kybic and M. Unser, "Fast parametric elastic image registration," *IEEE Trans. Image Process.*, vol. 12, no. 11, pp. 1427–1442, Nov. 2003.

[7] H. M. Chen, P. K. Varshney, and M. K. Arora, "Performance of mutual information similarity measure for registration of multitemporal remote sensing images," *IEEE Trans. Geosci. Remote Sens.*, vol. 41, no. 11, pp. 2445–2454, Nov. 2003.

[8] F. Wang and B. C. Vemuri, "Non-rigid multi-modal image registration using cross-cumulative residual entropy," *Int. J. Comput. Vis.*, vol. 74, no. 2, pp. 201–215, 2007.

[9] L. G. Brown, "A survey of image registration techniques," *ACM Comput. Surv.*, vol. 24, no. 4, pp. 325–376, 1992.

[10] R. Szeliski, "Image alignment and stitching: A tutorial," *Found. Trends Comput. Graph. Vis.*, vol. 2, no. 1, pp. 1–104, 2007.

[11] J. Le Moigne, N. S. Netanyahu, and R. D. Eastman, *Image Registration for Remote Sensing*. Cambridge, U.K.: Cambridge Univ. Press, 2011.

[12] A. A. Goshtasby, *Image Registration: Principles, Tools and Methods*. London, U.K.: Springer-Verlag, 2012.

[13] J. Le Moigne, "Introduction to remote sensing image registration," in *Proc. IEEE Int. Geosci. Remote Sens. Symp.*, Fort Worth, TX, USA, 2017, pp. 2565–2568.

[14] P. E. Anuta, "Spatial registration of multispectral and multitemporal digital imagery using fast Fourier transform techniques," *IEEE Trans. Geosci. Electron.*, vol. 8, no. 4, pp. 353–368, Oct. 1970.

[15] C. Kuglin, "The phase correlation image alignment method," in *Proc. Int. Conf. Cybern. Soc.*, 1975, pp. 163–165.

[16] A. Alba, J. F. Vigueras-Gomez, E. R. Arce-Santana, and R. M. Aguilar-Ponce, "Phase correlation with sub-pixel accuracy: A comparative study in 1D and 2D," *Comput. Vis. Image Understand.*, vol. 137, pp. 76–87, 2015.

[17] J. Ren, H. Zhao, J. Ren, and S. Cheng, "Sub-pixel motion estimation using phase correlation: Comparisons and evaluations," *Int. J. Intell. Comput. Cybern.*, vol. 9, no. 4, pp. 394–405, 2016.

[18] T. Heid and A. Kääb, "Evaluation of existing image matching methods for deriving glacier surface displacements globally from optical satellite imagery," *Remote Sens. Environ.*, vol. 118, pp. 339–355, 2012.

[19] G. Tzimiropoulos, V. Argyriou, S. Zafeiriou, and T. Stathaki, "Robust FFT-based scale-invariant image registration with image gradients," *IEEE Trans. Pattern Anal. Mach. Intell.*, vol. 32, no. 10, pp. 1899–1906, Oct. 2010.

[20] H. Foroosh, J. B. Zerubia, and M. Berthod, "Extension of phase correlation to subpixel registration," *IEEE Trans. Image Process.*, vol. 11, no. 3, pp. 188–200, Mar. 2002.

[21] J. L. Horner and P. D. Gianino, "Phase-only matched filtering," *Appl. Opt.*, vol. 23, no. 6, pp. 812–816, 1984.

[22] Q. Chen, M. Defrise, and F. Deconinck, "Symmetric phase-only matched filtering of Fourier-Mellin transforms for image registration and recognition," *IEEE Trans. Pattern Anal. Mach. Intell.*, vol. 16, no. 12, pp. 1156–1168, Dec.1994.

[23] S. Alliney and C. Morandi, "Digital image registration using projections," *IEEE Trans. Pattern Anal. Mach. Intell.*, vol. PAMI-8, no. 2, pp. 222–233, Mar. 1986.

[24] L. Hill and T. Vlachos, "Motion measurement using shape adaptive phase correlation," *Electron. Lett.*, vol. 37, no. 25, pp. 1512–1513, 2001.

[25] V. Argyriou and T. Vlachos, "Extrapolation-free arbitrary-shape motion estimation using phase correlation," *J. Electron. Imag.*, vol. 15, no. 1, 2006, Art. no. 010501.

[26] M. Li, M. Biswas, S. Kumar, and N. Truong, "DCT-based phase correlation motion estimation," in *Proc. Int. Conf. Image Process.*, Singapore, 2004, pp. 445–448.

[27] I. Ito and H. Kiya, "DCT sign-only correlation with application to image matching and the relationship with phase-only correlation," in *Proc. IEEE Int. Conf. Acoust. Signal Process.*, Honolulu, HI, USA, 2007, pp. I-1237–I-1240.

[28] V. Ojansivu and J. Heikkilä, "Image registration using blur-invariant phase correlation," *IEEE Signal Process. Lett.*, vol. 14, no. 7, pp. 449–452, Jul. 2007.

[29] M. Pedone, J. Flusser, and J. Heikkilä, "Blur invariant translational image registration for *N*-fold symmetric blurs," *IEEE Trans. Image Process.*, vol. 22, no. 9, pp. 3676–3689, Sep. 2013.

[30] M. Pedone, J. Flusser, and J. Heikkilä, "Registration of images with *N*-fold dihedral blur," *IEEE Trans. Image Process.*, vol. 24, no. 3, pp. 1036–1045, Mar. 2015.

[31] V. Argyriou, "Sub-hexagonal phase correlation for motion estimation," *IEEE Trans. Image Process.*, vol. 20, no. 1, pp. 110–120, Jan. 2011.

[32] D. Konstantinidis, T. Stathaki, and V. Argyriou, "Phase amplified correlation for improved sub-pixel motion estimation," *IEEE Trans. Image Process.*, vol. 28, no. 6, pp. 1–13, Jun. 2019.

[33] A. Alba and E. Arce-Santana, "Experimental evaluation of rigid registration using phase correlation under illumination changes," in *Proc. Int. Symp. Visual Comput.*, Las Vegas, NV, USA, 2015, pp. 151–161.

[34] X. Wan, J. Liu, and H. Yan, "The illumination robustness of phase correlation for image alignment," *IEEE Trans. Geosci. Remote Sens.*, vol. 53, no. 10, pp. 5746–5759, Oct. 2015.

[35] S. Yamaki, M. Abe, and M. Kawamata, "Statistical analysis of phase-only correlation functions based on directional statistics," *IEICE Trans. Fundam. Electron. Commun. Comput. Sci.*, vol. 97, no. 12, pp. 2601–2610, 2014.

[36] S. Yamaki, M. Abe, and M. Kawamata, "Statistical analysis of phase-only correlation functions with phase-spectrum differences following wrapped distributions," *IEICE Trans. Fundam. Electron. Commun. Comput. Sci.*, vol. 99, no. 10, pp. 1790–1798, 2016.

[37] S. Yamaki, M. Abe, and M. Kawamata, "Statistical analysis of phase-only correlation functions between real signals with stochastic phase-spectrum differences," *IEICE Trans. Fundam. Electron. Commun. Comput. Sci.*, vol. 100, no. 5, pp. 1097–1108, 2017.

[38] E. Gladilin and R. Eils, "On the role of spatial phase and phase correlation in vision, illusion, and cognition," *Front. Comput. Neurosci.*, vol. 9, 2015, Art. no. 45.

[39] S. J. Sangwine, T. A. Eli, and C. E. Moxey, "Vector phase correlation," *Electron. Lett.*, vol. 37, no. 25, pp. 1513–1515, 2001.

[40] C. E. Moxey, S. J. Sangwine, and T. A. Ell, "Hypercomplex correlation techniques for vector images," *IEEE Trans. Signal Process.*, vol. 51, no. 7, pp. 1941–1953, Jul. 2003.

[41] T. A. Ell and S. J. Sangwine, "Hypercomplex Fourier transforms of color images," *IEEE Trans. Image Process.*, vol. 16, no. 1, pp. 22–35, Jan. 2007.

[42] E. De Castro and C. Morandi, "Registration of translated and rotated images using finite Fourier transforms," *IEEE Trans. Pattern Anal. Mach. Intell.*, vol. PAMI-9, no. 5, pp. 700–703, Sep. 1987.

[43] B. S. Reddy and B. N. Chatterji, "An FFT-based technique for translation, rotation, and scale-invariant image registration," *IEEE Trans. Image Process.*, vol. 5, no. 8, pp. 1266–1271, Aug. 1996.

[44] H. S. Stone, B. Tao, and M. McGuire, "Analysis of image registration noise due to rotationally dependent aliasing," *J. Visual Commun. Image Representation*, vol. 14, no. 2, pp. 114–135, 2003.

[45] Y. Keller, A. Averbuch, and M. Israeli, "Pseudopolar-based estimation of large translations, rotations, and scalings in images," *IEEE Trans. Image Process.*, vol. 14, no. 1, pp. 12–22, Jan. 2005.

[46] H. Liu, B. Guo, and Z. Feng, "Pseudo-log-polar Fourier transform for image registration," *IEEE Signal Process. Lett.*, vol. 13, no. 1, pp. 17–20, Jan. 2006.

[47] A. Averbuch, R. R. Coifman, D. L. Donoho, M. Elad, and M. Israeli, "Fast and accurate polar Fourier transform," *Appl. Comput. Harmon. Anal.*, vol. 21, no. 2, pp. 145–167, 2006.

[48] W. Pan, K. Qin, and Y. Chen, "An adaptable-multilayer fractional Fourier transform approach for image registration," *IEEE Trans. Pattern Anal. Mach. Intell.*, vol. 31, no. 3, pp. 400–414, Mar. 2009.

[49] Z. Li, J. Yang, M. Li, and R. Lan, "Estimation of large scalings in images based on multilayer pseudopolar fractional Fourier transform," *Math. Probl. Eng.*, vol. 2013, 2013, Art. no. 179489.

[50] S. A. Abbas, Q. Sun, and H. Foroosh, "An exact and fast computation of discrete Fourier transform for polar and spherical grid," *IEEE Trans. Signal Process.*, vol. 65, no. 8, pp. 2033–2048, Apr. 2017.

[51] Y. Dong, W. Jiao, T. Long, G. He, and C. Gong, "An extension of phase correlation-based image registration to estimate similarity transform using multiple polar Fourier transform," *Remote Sens.*, vol. 10, no. 11, 2018, Art. no. 1719.

[52] Y. Keller, Y. Shkolnisky, and A. Averbuch, "The angular difference function and its application to image registration," *IEEE Trans. Pattern Anal. Mach. Intell.*, vol. 27, no. 6, pp. 969–976, Jun. 2005.

[53] T. Fujisawa and M. Ikehara, "High-accuracy image rotation and scale estimation using Radon transform and sub-pixel shift estimation," *IEEE Access*, vol. 7, pp. 22719–22728, 2019.

[54] L. Lucchese, "A frequency domain technique based on energy radial projections for robust estimation of global 2D affine transformations," *Comput. Vis. Image Understand.*, vol. 81, no. 1, pp. 72–116, 2001.

[55] L. Lucchese, S. Leorin, and G. M. Cortelazzo, "Estimation of two-dimensional affine transformations through polar curve matching and its application to image mosaicking and remote-sensing data registration," *IEEE Trans. Image Process.*, vol. 15, no. 10, pp. 3008–3019, Oct. 2006.

[56] L. Lucchese, G. Doretto, and G. M. Cortelazzo, "A frequency domain technique for range data registration," *IEEE Trans. Pattern Anal. Mach. Intell.*, vol. 24, no. 11, pp. 1468–1484, Nov. 2002.

[57] Y. Keller, Y. Shkolnisky, and A. Averbuch, "Volume registration using the 3-D pseudopolar Fourier transform," *IEEE Trans. Signal Process.*, vol. 54, no. 11, pp. 4323–4331, Nov. 2006.

[58] P. Curtis and P. Payeur, "A frequency domain approach to registration estimation in three-dimensional space," *IEEE Trans. Instrum. Meas.*, vol. 57, no. 1, pp. 110–120, Jan. 2008.

[59] J. Bican and J. Flusser, "3D Rigid registration by cylindrical phase correlation method," *Pattern Recognit. Lett.*, vol. 30, no. 10, pp. 914–921, 2009.

[60] H. Bülow and A. Birk, "Spectral 6DOF registration of noisy 3D range data with partial overlap," *IEEE Trans. Pattern Anal. Mach. Intell.*, vol. 35, no. 4, pp. 954–969, Apr. 2013.

[61] H. Bülow and A. Birk, "Scale-free registrations in 3D: 7 degrees of freedom with Fourier Mellin SOFT transforms," *Int. J. Comput. Vis.*, vol. 126, no. 7, pp. 731–750, 2018.

[62] A. HajiRassouliha, A. J. Taberner, M. P. Nash, and P. M. F. Nielsen, "Subpixel phase-based image registration using Savitzky-Golay differentiators in gradient-correlation," *Comput. Vis. Image Understand.*, vol. 170, pp. 28–39, 2018.

[63] L. Moisan, "Periodic plus smooth image decomposition," *J. Math. Imaging Vis.*, vol. 39, no. 2, pp. 161–179, 2011.

[64] J. Westerweel, "Fundamentals of digital particle image velocimetry," *Meas. Sci. Technol.*, vol. 8, no. 12, pp. 1379–1392, 1997.

[65] R. Michel and E. Rignot, "Flow of Glaciar Moreno, Argentina, from repeat-pass Shuttle Imaging Radar images: Comparison of the phase correlation method with radar interferometry," *J. Glaciol.*, vol. 45, no. 149, pp. 93–100, 1999.

[66] M. Druckmüller, "Phase correlation method for the alignment of total solar eclipse images," *Astrophys. J.*, vol. 706, no. 2, pp. 1605–1608, 2009.

[67] J. N. Caron, M. J. Montes, and J. L. Obermark, "Extracting flat-field images from scene-based image sequences using phase correlation," *Rev. Sci. Instrum.*, vol. 87, no. 6, 2016, Art. no. 063710.

[68] H. Nobach, N. Damaschke, and C. Tropea, "High-precision sub-pixel interpolation in particle image velocimetry image processing," *Exp. Fluids*, vol. 39, no. 2, pp. 299–304, 2005.

[69] M. Debella-Gilo and A. Kääb, "Sub-pixel precision image matching for measuring surface displacements on mass movements using normalized cross-correlation," *Remote Sens. Environ.*, vol. 115, no. 1, pp. 130–142, 2011.

[70] Q. Tian and M. N. Huhns, "Algorithms for subpixel registration," *Comput. Vis., Graph. Image Process.*, vol. 35, no. 2, pp. 220–233, 1986.

[71] I. E. Abdou, "Practical approach to the registration of multiple frames of video images," in *Proc. SPIE Conf. Vis. Commun. Image Process.*, 1999, pp. 371–382.

[72] V. Argyriou and T. Vlachos, "Estimation of sub-pixel motion using gradient cross-correlation," *Electron. Lett.*, vol. 39, no. 13, pp. 980–982, 2003.

[73] A. C. Eckstein, J. Charonko, and P. Vlachos, "Phase correlation processing for DPIV measurements," *Exp. Fluids*, vol. 45, no. 3, pp. 485–500, 2008.

[74] J. Ren, T. Vlachos, Y. Zhang, J. Zheng, and J. Jiang, "Gradient-based subspace phase correlation for fast and effective image alignment," *J. Vis. Commun. Image R.*, vol. 25, no. 7, pp. 1558–1565, 2014.

[75] J. Li, Y. Liu, S. Du, P. Wu, and Z. Xu, "Hierarchical and adaptive phase correlation for precise disparity estimation of UAV images," *IEEE Trans. Geosci. Remote Sens.*, vol. 54, no. 12, pp. 7092–7104, Dec. 2016.

[76] C. Lynch and N. Devaney, "Registration for images in the presence of additive and multiplicative fixed-pattern noise," *Appl. Opt.*, vol. 57, no. 8, pp. 1824–1831, 2018.

[77] S. Nagashima, T. Aoki, T. Higuchi, and K. Kobayashi, "A subpixel image matching technique using phase-only correlation," in *Proc. Int. Symp. Intell. Signal Process. Commun. Syst.*, Tottori, Japan, 2006, pp. 701–704.

[78] L. Chen and K. H. Yap, "An effective technique for subpixel image registration under noisy conditions," *IEEE Trans. Syst., Man, Cybern. A*, vol. 38, no. 4, pp. 881–887, Jul. 2008.

[79] J. Ren, J. Jiang, and T. Vlachos, "High-accuracy sub-pixel motion estimation from noisy images in Fourier domain," *IEEE Trans. Image Process.*, vol. 19, no. 5, pp. 1379–1384, May 2010.

[80] N. Ma, P.-F. Sun, Y.-B. Men, C.-G. Men, and X. Li, "A subpixel matching method for stereovision of narrow baseline remotely sensed imagery," *Math. Probl. Eng.*, vol. 2017, 2017, Art. no. 7901692.

[81] K. Takita, T. Aoki, Y. Sasaki, T. Higuchi, and K. Kobayashi, "High-accuracy subpixel image registration based on phase-only correlation," *IEICE Trans. Fundam. Electron. Commun. Comput. Sci.*, vol. 86, no. 8, pp. 1925–1934, 2003.

[82] K. Takita, M. A. Muquit, and T. Higuchi, "A sub-pixel correspondence search technique for computer vision applications," *IEICE Trans. Fundam. Electron. Commun. Comput. Sci.*, vol. 87, no. 8, pp. 1913–1923, 2004.

[83] J. Chen, W. Xu, H. Xu, F. Lin, Y. Sun, and X. Shi, "Fast vehicle detection using a disparity projection method," *IEEE Trans. Intell. Transp. Syst.*, vol. 19, no. 9, pp. 2801–2813, Sep. 2018.

[84] V. Argyriou and T. Vlachos, "On the estimation of subpixel motion using phase correlation," *J. Electron. Imag.*, vol. 16, no. 3, 2007, Art. no. 033018.

[85] Y. Wang and C. Yan, "Sub-pixel image registration of spectrometer images," *Opt. Precision Eng.*, vol. 20, no. 3, pp. 661–667, 2012.

[86] G. Tzimiropoulos, V. Argyriou, and T. Stathaki, "Subpixel registration with gradient correlation," *IEEE Trans. Image Process.*, vol. 20, no. 6, pp. 1761–1767, Jun. 2011.

[87] V. Argyriou and G. Tzimiropoulos, "Frequency domain subpixel registration using HOG phase correlation," *Comput. Vis. Image Understand.*, vol. 155, pp. 70–82, 2017.

[88] Z. Ye *et al.*, "Illumination-robust subpixel Fourier-based image correlation methods based on phase congruency," *IEEE Trans. Geosci. Remote Sens.*, vol. 57, no. 4, pp. 1995–2008, Apr. 2019.

[89] S. S. Young and R. G. Driggers, "Superresolution image reconstruction from a sequence of aliased imagery," *Appl. Opt.*, vol. 45, no. 21, pp. 5073–5085, 2006.

[90] X. Zhang, M. Abe, and M. Kawamata, "Reduction of computational cost of POC-based methods for displacement estimation in old film sequences," *IEICE Trans. Fundam. Electron. Commun. Comput. Sci.*, vol. E94-A, no. 7, pp. 1497–1504, 2011.

[91] M. Guizar-Sicairos, S. T. Thurman, and J. R. Fienup, "Efficient subpixel image registration algorithms," *Opt. Lett.*, vol. 33, no. 2, pp. 156–158, 2008.

[92] C. Wang, X. Jing, and C. Zhao, "Local upsampling Fourier transform for accurate 2D/3D image registration," *Comput. Electr. Eng.*, vol. 38, no. 5, pp. 1346–1357, 2012.

[93] A. Yousef, J. Li, and M. Karim, "High-speed image registration algorithm with subpixel accuracy," *IEEE Signal Process. Lett.*, vol. 22, no. 10, pp. 1796–1800, Oct. 2015.

[94] T. Roesgen, "Optimal subpixel interpolation in particle image velocimetry," *Exp. Fluids*, vol. 35, no. 3, pp. 252–256, 2003.

[95] H. S. Stone, M. T. Orchard, E.-C. Chang, and S. A. Martucci, "A fast direct Fourier-based algorithm for subpixel registration of images," *IEEE Trans. Geosci. Remote Sens.*, vol. 39, no. 10, pp. 2235–2243, Oct. 2001.

[96] D. T. K. Malcolm, P. M. F. Nielsen, P. J. Hunter, and P. G. Charette, "Strain measurement in biaxially loaded inhomogeneous, anisotropic elastic membranes," *Biomech. Model. Mechanobiol.*, vol. 1, no. 3, pp. 197–210, 2002.

[97] A. Averbuch and Y. Keller, "FFT based image registration," in *Proc. IEEE Int. Conf. Acoust., Speech Signal Process.*, Orlando, FL, USA, 2002, pp. IV-3608–IV-3611.

[98] P. Vandewalle, S. Sü, and M. Vetterli, "A frequency domain approach to registration of aliased images with application to super-resolution," *EURASIP J. Appl. Signal Process.*, vol. 2006, 2006, Art. no. 071459.

[99] J. Liu and H. Yan, "Phase correlation pixel-to-pixel image co-registration based on optical flow and median shift propagation," *Int. J. Remote Sens.*, vol. 29, no. 20, pp. 5943–5956, 2008.

[100] P. J. González, M. Chini, S. Stramondo, and J. Fernández, "Coseismic horizontal offsets and fault-trace mapping using phase correlation of IRS satellite images: The 1999 Izmit (Turkey) earthquake," *IEEE Trans. Geosci. Remote Sens.*, vol. 48, no. 5, pp. 2242–2250, May 2010.

[101] G. L. K. Morgan, J. Liu, and H. Yan, "Precise subpixel disparity measurement from very narrow baseline stereo," *IEEE Trans. Geosci. Remote Sens.*, vol. 48, no. 9, pp. 3424–3433, Sep. 2010.

[102] B. He, G. Wang, X. Lin, C. Shi, and C. Liu, "High-accuracy sub-pixel registration for noisy images based on phase correlation," *IEICE Trans. Inf. Syst.*, vol. E94D, no. 12, pp. 2541–2544, 2011.

[103] X. Tong *et al.*, "An improved phase correlation method based on 2-D plane fitting and the maximum kernel density estimator," *IEEE Geosci. Remote Sens. Lett.*, vol. 12, no. 9, pp. 1953–1957, Sep. 2015.

[104] Z. Ye *et al.*, "An improved subpixel phase correlation method with application in videogrammetric monitoring of shaking table tests," *Photogramm. Eng. Remote Sens.*, vol. 84, no. 9, pp. 579–592, 2018.

[105] W. S. Hoge, "A subspace identification extension to the phase correlation method [MRI application]," *IEEE Trans. Med. Imag.*, vol. 22, no. 2, pp. 277–280, Feb. 2003.

[106] H. Foroosh and M. Balci, "Sub-pixel registration and estimation of local shifts directly in the Fourier domain," in *Proc. Int. Conf. Image Process.*, 2004, pp. 1915–1918.

[107] W. S. Hoge and C. F. Westin, "Identification of translational displacements between N-dimensional data sets using the high-order SVD and phase correlation," *IEEE Trans. Image Process.*, vol. 14, no. 7, pp. 884–889, Jul. 2005.

[108] Y. Keller and A. Averbuch, "A projection-based extension to phase correlation image alignment," *Signal Process.*, vol. 87, no. 1, pp. 124–133, 2007.

[109] R. S. J. Estépar, C.-F. Westin, and K. G. Vosburgh, "Towards real time 2D to 3D registration for ultrasound-guided endoscopic and laparoscopic procedures," *Int. J. Comput. Assist. Radiol. Surg.*, vol. 4, no. 6, pp. 549–560, 2009.

[110] X. Tong *et al.*, "A novel subpixel phase correlation method using singular value decomposition and unified random sample consensus," *IEEE Trans. Geosci. Remote Sens.*, vol. 53, no. 8, pp. 4143–4156, Aug. 2015.

[111] H. Wang, J. Zhao, J. Zhao, F. Dong, Z. Pan, and Y. Feng, "Position detection method of linear motor mover based on extended phase correlation algorithm," *IET Sci. Meas. Technol.*, vol. 11, no. 7, pp. 921–928, 2017.

[112] Z. Chen, B. Liu, S. Wang, and E. Liu, "Efficient subpixel registration for polarization-modulated 3D imaging," *Opt. Express*, vol. 26, no. 18, pp. 23040–23050, 2018.

[113] Y. Dong, T. Long, W. Jiao, G. He, and Z. Zhang, "A novel image registration method based on phase correlation using low-rank matrix factorization with mixture of Gaussian," *IEEE Trans. Geosci. Remote Sens.*, vol. 56, no. 1, pp. 446–460, Jan. 2018.

[114] M. Balci and H. Foroosh, "Subpixel estimation of shifts directly in the Fourier domain," *IEEE Trans. Image Process.*, vol. 15, no. 7, pp. 1965–1972, Jul. 2006.

[115] M. Balci and H. Foroosh, "Subpixel registration directly from the phase difference," *EURASIP J. Appl. Signal Process.*, vol. 2006, 2006, Art. no. 060796.

[116] C. Zuo, Q. Chen, G. Gu, and X. Sui, "Registration method for infrared images under conditions of fixed-pattern noise," *Opt. Commun.*, vol. 285, no. 9, pp. 2293–2302, 2012.

[117] M. Xu and P. K. Varshney, "A subspace method for Fourier-based image registration," *IEEE Geosci. Remote Sens. Lett.*, vol. 6, no. 3, pp. 491–494, Jul. 2009.

[118] S. P. Kim and W.-Y. Su, "Subpixel accuracy image registration by spectrum cancellation," in *Proc. IEEE Int. Conf. Acoust., Speech Signal Process.*, Minneapolis, MN, USA, 1993, pp. 153–156.

[119] N. Van Puymbroeck, R. Michel, R. Binet, J.-P. Avouac, and J. Taboury, "Measuring earthquakes from optical satellite images," *Appl. Opt.*, vol. 39, no. 20, pp. 3486–3494, 2000.

[120] S. Leprince, S. Barbot, F. Ayoub, and J.-P. Avouac, "Automatic and precise orthorectification, coregistration, and subpixel correlation of satellite images, application to ground deformation measurements," *IEEE Trans. Geosci. Remote Sens.*, vol. 45, no. 6, pp. 1529–1558, Jun. 2007.

[121] J. R. Fienup, "Invariant error metrics for image reconstruction," *Appl. Opt.*, vol. 36, no. 32, pp. 8352–8357, 1997.

[122] X. Li, "An improved two-stage image registration algorithm for super-resolution," *IEEJ Trans. Electr. Electron. Eng.*, vol. 9, no. 4, pp. 415–420, 2014.

[123] C. Zhou, J. Zhu, D. Fan, and J. Zhou, "An improved algorithm of image registration based on least squares adjustment," *Surv. Rev.*, vol. 48, no. 349, pp. 240–246, 2016.

[124] B. Pan, Y. Wang, and L. Tian, "Automated initial guess in digital image correlation aided by Fourier-Mellin transform," *Opt. Eng.*, vol. 56, no. 1, 2017, Art. no. 014103.

[125] Y. Douini, J. Riffi, A. M. Mahraz, and H. Tairi, "An image registration algorithm based on phase correlation and the classical Lucas–Kanade technique," *Signal Image Video Process.*, vol. 11, no. 7, pp. 1321–1328, 2017.

[126] X. Li, "High-accuracy subpixel image registration with large displacements," *IEEE Trans. Geosci. Remote Sens.*, vol. 55, no. 11, pp. 6265–6276, Nov. 2017.

[127] Z. Zhao, X. Feng, S. Teng, Y. Li, and C. Zhang, "Multiscale point correspondence using feature distribution and frequency domain alignment," *Math. Problems Eng.*, vol. 2012, 2012, Art. no. 382369.

[128] H. Li, A. Zhang, and S. Hu, "A registration scheme for multispectral systems using phase correlation and scale invariant feature matching," *J. Sensors*, vol. 2016, 2016, Art. no. 3789570.

[129] H. Li and Y. Man, "Robust multi-source image registration for optical satellite based on phase information," *Photogramm. Eng. Remote Sens.*, vol. 82, no. 11, pp. 865–878, 2016.

[130] C. A. Wilson and J. A. Theriot, "A correlation-based approach to calculate rotation and translation of moving cells," *IEEE Trans. Image Process.*, vol. 15, no. 7, pp. 1939–1951, Jul. 2006.

[131] H. Bülow and A. Birk, "Spectral registration of noisy sonar data for underwater 3D mapping," *Auton. Robot.*, vol. 30, no. 3, pp. 307–331, 2011.

[132] N. Hurtós, D. Ribas, X. Cufí, Y. Petillot, and J. Salvi, "Fourier-based registration for robust forward-looking sonar mosaicing in low-visibility underwater environments," *J. Field Robot.*, vol. 32, no. 1, pp. 123–151, 2015.

[133] R. Abdelfattah and J. M. Nicolas, "InSAR image co-registration using the Fourier-Mellin transform," *Int. J. Remote Sens.*, vol. 26, no. 13, pp. 2865–2876, 2005.

[134] H. Erives and G. J. Fitzgerald, "Automatic subpixel registration for a tunable hyperspectral imaging system," *IEEE Geosci. Remote Sens. Lett.*, vol. 3, no. 3, pp. 397–400, Jul. 2006.

[135] D. Scheffler, A. Hollstein, H. Diedrich, K. Segl, and P. Hostert, "AROSICS: An automated and robust open-source image co-registration software for multi-sensor satellite data," *Remote Sens.*, vol. 9, no. 7, 2017, Art. no. 676.

[136] D. Hong, W. Liu, J. Su, Z. Pan, and G. Wang, "A novel hierarchical approach for multispectral palmprint recognition," *Neurocomputing*, vol. 151, pp. 511–521, 2015.

[137] K. Ito, H. Nakajima, K. Kobayashi, and T. Higuchi, "A fingerprint matching algorithm using phase-only correlation," *IEICE Trans. Fundam. Electron. Commun. Comput. Sci.*, vol. 87, no. 3, pp. 682–691, 2004.

[138] K. Miyazawa, K. Ito, T. Aoki, K. Kobayashi, and H. Nakajima, "An effective approach for iris recognition using phase-based image matching," *IEEE Trans. Pattern Anal. Mach. Intell.*, vol. 30, no. 10, pp. 1741–1756, Oct. 2008.

[139] L. Zhang, L. Zhang, D. Zhang, and H. Zhu, "Ensemble of local and global information for finger-knuckle-print recognition," *Pattern Recognit.*, vol. 44, no. 9, pp. 1990–1998, 2011.

[140] D. Rizo-Rodríguez, H. Méndez-Vázquez, and E. García-Reyes, "Illumination invariant face recognition using quaternion-based correlation filters," *J. Math. Imaging Vis.*, vol. 45, no. 2, pp. 164–175, 2013.

[141] M. S. Mohd Asaari, S. A. Suandi, and B. A. Rosdi, "Fusion of band limited phase only correlation and width centroid contour distance for finger based biometrics," *Expert Syst. Appl.*, vol. 41, no. 7, pp. 3367–3382, 2014.

[142] I. Rida, S. Almaadeed, and A. Bouridane, "Gait recognition based on modified phase-only correlation," *Signal Image Video Process*., vol. 10, no. 3, pp. 463–470, 2016.

[143] A. Kumar, "Toward more accurate matching of contactless palmprint images under less constrained environments," *IEEE Trans. Inf. Forensic Secur.*, vol. 14, no. 1, pp. 34–47, Jan. 2019.

[144] H. Moriya, "Phase-only correlation of time-varying spectral representations of microseismic data for identification of similar seismic events," *Geophysics*, vol. 76, no. 6, pp. WC37–WC45, 2011.

[145] G. Tomar, S. C. Singh, and J. P. Montagner, "Sub-sample time shift and horizontal displacement measurements using phase-correlation method in time-lapse seismic," *Geophys. Prospect.*, vol. 65, no. 2, pp. 407–425, 2017.

[146] J. Jang, Y. Yoo, J. Kim, and J. Paik, "Sensor-based auto-focusing system using multi-scale feature extraction and phase correlation matching," *Sensors*, vol. 15, no. 3, pp. 5747–5762, 2015.

[147] S. Ertürk, "Digital image stabilization with sub-image phase correlation based global motion estimation," *IEEE Trans. Consum. Electron.*, vol. 49, no. 4, pp. 1320–1325, Nov. 2003.

[148] Q. Wu, S. Wang, and X. Zhang, "Log-polar based scheme for revealing duplicated regions in digital images," *IEEE Signal Process. Lett.*, vol. 18, no. 10, pp. 559–562, Oct. 2011.

[149] D. Zheng, J. Zhao, and A. E. Saddik, "RST-invariant digital image watermarking based on log-polar mapping and phase correlation," *IEEE Trans. Circuits Syst. Video Technol.*, vol. 13, no. 8, pp. 753–765, Aug. 2003.

[150] C. Zuo, Q. Chen, G. Gu, and X. Sui, "Scene-based nonuniformity correction algorithm based on interframe registration," *J. Opt. Soc. Amer. A*, vol. 28, no. 6, pp. 1164–1176, 2011.

[151] Y. Keller and Y. Shkolnisky, "A signal processing approach to symmetry detection," *IEEE Trans. Image Process.*, vol. 15, no. 8, pp. 2198–2207, Aug. 2006.

[152] T. Vlachos, "Cut detection in video sequences using phase correlation," *IEEE Signal Process. Lett.*, vol. 7, no. 7, pp. 173–175, Jul. 2000.

[153] C. Dai, Y. Zheng, and X. Li, "Accurate video alignment using phase correlation," *IEEE Signal Process. Lett.*, vol. 13, no. 12, pp. 737–740, Dec. 2006.

[154] M. Paul, W. Lin, C. T. Lau, and B.-S. Lee, "Direct intermode selection for H. 264 video coding using phase correlation," *IEEE Trans. Image Process.*, vol. 20, no. 2, pp. 461–473, Feb. 2011.

[155] M. Barkowsky, J. Bialkowski, B. Eskofier, R. Bitto, and A. Kaup, "Temporal trajectory aware video quality measure," *IEEE J. Sel. Topics Signal Process.*, vol. 3, no. 2, pp. 266–279, Apr. 2009.

[156] G. Miyamoto, A. Shibata, T. Maki, and T. Furuhara, "Precise measurement of strain accommodation in austenite matrix surrounding martensite in ferrous alloys by electron backscatter diffraction analysis," *Acta Materialia*, vol. 57, no. 4, pp. 1120–1131, 2009.

[157] V. Rubino, N. Lapusta, A. J. Rosakis, S. Leprince, and J. P. Avouac, "Static laboratory earthquake measurements with the digital image correlation method," *Exp. Mech.*, vol. 55, no. 1, pp. 77–94, 2015.

[158] D. J. Kelly, E. U. Azeloglu, P. V. Kochupura, G. S. Sharma, and G. R. Gaudette, "Accuracy and reproducibility of a subpixel extended phase correlation method to determine micron level displacements in the heart," *Med. Eng. Phys.*, vol. 29, no. 1, pp. 154–162, 2007.

[159] D. Teyssieux, S. Euphrasie, and B. Cretin, "MEMS in-plane motion/vibration measurement system based CCD camera," *Measurement*, vol. 44, no. 10, pp. 2205–2216, 2011.

[160] Q. Yang, S. Jagannathan, and E. W. Bohannan, "Automatic drift compensation using phase correlation method for nanomanipulation," *IEEE Trans. Nanotechnol.*, vol. 7, no. 2, pp. 209–216, Mar. 2008.

[161] N. Marturi, B. Tamadazte, S. Dembélé, and N. Piat, "Image-guided nanopositioning scheme for SEM," *IEEE Trans. Autom. Sci. Eng.*, vol. 15, no. 1, pp. 45–56, Jan. 2018.

[162] M. Thomas, S. Misra, C. Kambhamettu, and J. T. Kirby, "A robust motion estimation algorithm for PIV," *Meas. Sci. Technol.*, vol. 16, no. 3, pp. 865–877, 2005.

[163] D. Feng, M. Q. Feng, E. Ozer, and Y. Fukuda, "A vision-based sensor for noncontact structural displacement measurement," *Sensors*, vol. 15, no. 7, 2015, Art. no. 16557.

[164] F. Morbidi and G. Caron, "Phase correlation for dense visual compass from omnidirectional camera-robot images," *IEEE Robot. Autom. Lett.*, vol. 2, no. 2, pp. 688–695, Apr. 2017.

[165] L. Zhang, D. Bi, Y. Zha, S. Gao, H. Wang, and T. Ku, "Robust and fast visual tracking via spatial kernel phase correlation filter," *Neurocomputing*, vol. 204, pp. 77–86, 2016.

[166] D. Hong, N. Yokoya, J. Chanussot, and X. X. Zhu, "An augmented linear mixing model to address spectral variability for hyperspectral unmixing," *IEEE Trans. Image Process.*, vol. 28, no. 4, pp. 1923–1938, Apr. 2019.

[167] A. Ertürk and S. Ertürk, "Unsupervised segmentation of hyperspectral images using modified phase correlation," *IEEE Geosci. Remote Sens. Lett.*, vol. 3, no. 4, pp. 527–531, Oct. 2006.

[168] B. Demir and S. Ertürk, "Phase correlation based redundancy removal in feature weighting band selection for hyperspectral images," *Int. J. Remote Sens.*, vol. 29, no. 6, pp. 1801–1807, 2008.

[169] D. Çeşmeci and M. K. Güllü, "Phase-correlation-based hyperspectral image classification using multiple class representatives obtained with k-means clustering," *Int. J. Remote Sens.*, vol. 30, no. 14, pp. 3827–3834, 2009.

[170] Y. Jiang, G. Zhang, X.-M. Tang, D. Li, W. Huang, and H.-B. Pan, "Geometric calibration and accuracy assessment of ZiYuan-3 multispectral images," *IEEE Trans. Geosci. Remote Sens.*, vol. 52, no. 7, pp. 4161–4172, Jul. 2014.

[171] A. Fitch, A. Kadyrov, W. J. Christmas, and J. Kittler, "Orientation correlation," in *Proc. Brit. Mach. Vision Conf.*, 2002, pp. 133–142.

[172] M. H. Taylor, S. Leprince, J.-P. Avouac, and K. Sieh, "Detecting coseismic displacements in glaciated regions: An example from the great November 2002 Denali earthquake using SPOT horizontal offsets," *Earth Planet. Sci. Lett.*, vol. 270, no. 3, pp. 209–220, 2008.

[173] A. Dehecq, N. Gourmelen, and E. Trouve, "Deriving large-scale glacier velocities from a complete satellite archive: Application to the Pamir-Karakoram-Himalaya," *Remote Sens. Environ.*, vol. 162, pp. 55–66, 2015.

[174] D. Scherler, S. Leprince, and M. R. Strecker, "Glacier-surface velocities in alpine terrain from optical satellite imagery—Accuracy improvement and quality assessment," *Remote Sens. Environ.*, vol. 112, no. 10, pp. 3806–3819, 2008.

[175] L. Fang, Y. Xu, W. Yao, and U. Stilla, "Estimation of glacier surface motion by robust phase correlation and point like features of SAR intensity images," *ISPRS J. Photogramm. Remote Sens.*, vol. 121, pp. 92–112, 2016.

[176] A. Lucieer, S. M. de Jong, and D. Turner, "Mapping landslide displacements using Structure from Motion (SfM) and image correlation of multi-temporal UAV photography," *Prog. Phys. Geogr.*, vol. 38, no. 1, pp. 97–116, 2013.

[177] P. Lacroix, E. Berthier, and E. T. Maquerhua, "Earthquake-driven acceleration of slow-moving landslides in the Colca valley, Peru, detected from Pléiades images," *Remote Sens. Environ.*, vol. 165, pp. 148–158, 2015.

[178] M. Necsoiu, S. Leprince, D. M. Hooper, C. L. Dinwiddie, R. N. McGinnis, and G. R. Walter, "Monitoring migration rates of an active subarctic dune field using optical imagery," *Remote Sens. Environ.*, vol. 113, no. 11, pp. 2441–2447, 2009.

[179] N. Bridges, F. Ayoub, J. Avouac, S. Leprince, A. Lucas, and S. Mattson, "Earth-like sand fluxes on Mars," *Nature*, vol. 485, no. 7398, pp. 339–342, 2012.

[180] M. de Michele, S. Leprince, J. Thiébot, D. Raucoules, and R. Binet, "Direct measurement of ocean waves velocity field from a single SPOT-5 dataset," *Remote Sens. Environ.*, vol. 119, pp. 266–271, 2012.

[181] M. de Michele, D. Raucoules, and Þ. Arason, "Volcanic plume elevation model and its velocity derived from Landsat 8," *Remote Sens. Environ.*, vol. 176, pp. 219–224, 2016.

[182] M. Thomas, C. Kambhamettu, and C. A. Geiger, "Motion tracking of discontinuous sea ice," *IEEE Trans. Geosci. Remote Sens.*, vol. 49, no. 12, pp. 5064–5079, Dec. 2011.

[183] A. Berg and L. E. B. Eriksson, "Investigation of a hybrid algorithm for sea ice drift measurements using synthetic aperture radar images," *IEEE Trans. Geosci. Remote Sens.*, vol. 52, no. 8, pp. 5023–5033, Aug. 2014.

[184] A. Iwasaki, "Detection and estimation of satellite attitude jitter using remote sensing imagery," in *Advances in Spacecraft Technologies*, J. Hall, ed. Rijeka, Croatia: InTech, 2011, pp. 257–272.

[185] X. Tong *et al.*, "Framework of jitter detection and compensation for high resolution satellites," *Remote Sens.*, vol. 6, no. 5, pp. 3944–3964, 2014.

[186] H. Pan, Z. Zou, G. Zhang, X. Zhu, and X. Tang, "A penalized spline-based attitude model for high-resolution satellite imagery," *IEEE Trans. Geosci. Remote Sens.*, vol. 54, no. 3, pp. 1849–1859, Mar. 2016.

[187] J. E. Pardo-Pascual, J. Almonacid-Caballer, L. A. Ruiz, and J. Palomar-Vázquez, "Automatic extraction of shorelines from Landsat TM and ETM+ multi-temporal images with subpixel precision," *Remote Sens. Environ.*, vol. 123, pp. 1–11, 2012.

[188] R. Mumtaz, P. Palmer, and M. Waqar, "Georeferencing of UK DMC stereo-images without ground control points by exploiting geometric distortions," *Int. J. Remote Sens.*, vol. 35, no. 6, pp. 2136–2169, 2014.

[189] A. Kääb and S. Leprince, "Motion detection using near-simultaneous satellite acquisitions," *Remote Sens. Environ.*, vol. 154, pp. 164–179, 2014.

[190] X. Wan, J. Liu, H. Yan, and G. L. K. Morgan, "Illumination-invariant image matching for autonomous UAV localisation based on optical sensing," *ISPRS J. Photogramm. Remote Sens.*, vol. 119, pp. 198–213, 2016.

[191] S. Leprince, P. Musé, and J.-P. Avouac, "In-flight CCD distortion calibration for pushbroom satellites based on subpixel correlation," *IEEE Trans. Geosci. Remote Sens.*, vol. 46, no. 9, pp. 2675–2683, Sep. 2008.

[192] N. Yokoya, N. Miyamura, and A. Iwasaki, "Detection and correction of spectral and spatial misregistrations for hyperspectral data using phase correlation method," *Appl. Opt.*, vol. 49, no. 24, pp. 4568–4575, 2010.

[193] Y. Dong, W. Chen, H. Chang, Y. Zhang, R. Feng, and L. Meng, "Assessment of orthoimage and DEM derived from ZY-3 stereo image in Northeastern China," *Surv. Rev.*, vol. 48, no. 349, pp. 247–257, 2016.

[194] Á. Ordóñez, F. Argüello, and D. B. Heras, "Fourier-Mellin registration of two hyperspectral images," *Int. J. Remote Sens.*, vol. 38, no. 11, pp. 3253–3273, 2017.

[195] Á. Ordóñez, F. Argüello, and D. B. Heras, "GPU accelerated FFT-based registration of hyperspectral scenes," *IEEE J. Sel. Topics Appl. Earth Observ. Remote Sens.*, vol. 10, no. 11, pp. 4869–4878, Nov. 2017.

[196] R. Kolar, V. Harabis, and J. Odstrcilik, "Hybrid retinal image registration using phase correlation," *Imag. Sci. J.*, vol. 61, no. 4, pp. 369–384, 2013.

[197] G. Vaillant, C. Prieto, C. Kolbitsch, G. Penney, and T. Schaeffter, "Retrospective rigid motion correction in k-space for segmented radial MRI," *IEEE Trans. Med. Imag.*, vol. 33, no. 1, pp. 1–10, Jan. 2014.

[198] S. Skakun, J.-C. Roger, E. F. Vermote, J. G. Masek, and C. O. Justice, "Automatic sub-pixel co-registration of Landsat-8 Operational Land Imager and Sentinel-2A Multi-Spectral Instrument images using phase correlation and machine learning based mapping," *Int. J. Digit. Earth*, vol. 10, no. 12, pp. 1253–1269, 2017.

[199] M. Henke, A. Junker, K. Neumann, T. Altmann, and E. Gladilin, "Automated alignment of multi-modal plant images using integrative phase correlation approach," *Front. Plant Sci.*, vol. 9, 2018, Art. no. 1519.

[200] H. Li, J. Luo, C. Huang, Y. Yang, and S. Xie, "An adaptive image-stitching algorithm for an underwater monitoring system," *Int. J. Adv. Robot. Syst.*, vol. 11, no. 10, 2014, Art. no. 166.

[201] M. A. Muquit, T. Shibahara, and T. Aoki, "A high-accuracy passive 3D measurement system using phase-based image matching," *IEICE Trans. Fundam. Electron. Commun. Comput. Sci.*, vol. 89, no. 3, pp. 686–697, 2006.

[202] S. Wu, Y. Wang, Y. Zhan, and X. Chang, "Automatic microseismic event detection by band-limited phase-only correlation," *Phys. Earth Planet. Inter.*, vol. 261, pp. 3–16, 2016.

[203] S. Kumar, H. Azartash, M. Biswas, and T. Nguyen, "Real-time affine global motion estimation using phase correlation and its application for digital image stabilization," *IEEE Trans. Image Process.*, vol. 20, no. 12, pp. 3406–3418, Dec. 2011.

[204] H. Shao, T. Yu, M. Xu, and W. Cui, "Image region duplication detection based on circular window expansion and phase correlation," *Forensic Sci. Int.*, vol. 222, no. 1, pp. 71–82, 2012.

[205] X. Kang, J. Huang, and W. Zeng, "Efficient general print-scanning resilient data hiding based on uniform log-polar mapping," *IEEE Trans. Inf. Forensic Secur.*, vol. 5, no. 1, pp. 1–12, Mar. 2010.

[206] J. Ouyang, G. Coatrieux, B. Chen, and H. Shu, "Color image watermarking based on quaternion Fourier transform and improved uniform log-polar mapping," *Comput. Electr. Eng.*, vol. 46, pp. 419–432, 2015.

[207] N. Liu and J. Xie, "Interframe phase-correlated registration scene-based nonuniformity correction technology," *Infrared Phys. Technol.*, vol. 69, pp. 198–205, 2015.

[208] G. Tzimiropoulos, V. Argyriou, and T. Stathaki, "Symmetry detection using frequency domain motion estimation techniques," in *Proc. IEEE Int. Conf. Acoust., Speech Signal Process.*, Las Vegas, NV, USA, 2008, pp. 861–864.

[209] O. Urhan, M. K. Gullu, and S. Erturk, "Modified phase-correlation based robust hard-cut detection with application to archive film," *IEEE Trans. Circuits Syst. Video Technol.*, vol. 16, no. 6, pp. 753–770, Jun. 2006.

[210] J. Jia, Y.-W. Tai, T.-P. Wu, and C.-K. Tang, "Video repairing under variable illumination using cyclic motions," *IEEE Trans. Pattern Anal. Mach. Intell.*, vol. 28, no. 5, pp. 832–839, May 2006.

[211] A. Mittal, S. Gupta, S. Jain, and A. Jain, "Content-based adaptive compression of educational videos using phase correlation techniques," *Multimedia Syst.*, vol. 11, no. 3, pp. 249–259, 2006.

[212] Y. Ismail, M. A. Elgamel, and M. A. Bayoumi, "Fast variable padding motion estimation using smart zero motion prejudgment technique for pixel and frequency domains," *IEEE Trans. Circuits Syst. Video Technol.*, vol. 19, no. 5, pp. 609–626, 2009.

[213] T. Riedl and H. Wendrock, "Reliability of high-resolution electron backscatter diffraction determination of strain and rotation variations using phase-only and cross correlation," *Cryst. Res. Technol.*, vol. 49, no. 4, pp. 195–203, 2014.

[214] Y. Caniven *et al.*, "A new multilayered visco-elasto-plastic experimental model to study strike-slip fault seismic cycle," *Tectonics*, vol. 34, no. 2, pp. 232–264, 2015.

[215] A. de Oliveira, J. Rauschenberg, D. Beyersdorff, W. Semmler, and M. Bock, "Automatic passive tracking of an endorectal prostate biopsy device using phase-only cross-correlation," *Magn. Reson. Med.*, vol. 59, no. 5, pp. 1043–1050, 2008.

[216] A. J. Krafft *et al.*, "Passive marker tracking via phase-only cross correlation (POCC) for MR-guided needle interventions: Initial in vivo experience," *Physica Medica*, vol. 29, no. 6, pp. 607–614, 2013.

[217] B. Serio, J. J. Hunsinger, and B. Cretin, "In-plane measurements of microelectromechanical systems vibrations with nanometer resolution using the correlation of synchronous images," *Rev. Sci. Instrum.*, vol. 75, no. 10, pp. 3335–3341, 2004.

[218] C. Recknagel and H. Rothe, "A concept for automated nanoscale atomic force microscope (AFM) measurements using a priori knowledge," *Meas. Sci. Technol.*, vol. 20, no. 8, 2009, Art. no. 084026.

[219] P. Cizmar, A. E. Vladár, and M. T. Postek, "Real-time scanning charged-particle microscope image composition with correction of drift," *Microsc. Microanal.*, vol. 17, no. 2, pp. 302–308, 2011.
[220] A. Eckstein and P. P. Vlachos, "Digital particle image velocimetry (DPIV) robust phase correlation," *Meas. Sci. Technol.*, vol. 20, no. 5, 2009, Art. no. 055401.
[221] J. S. Raben, S. A. Klein, J. D. Posner, and P. P. Vlachos, "Improved accuracy of time-resolved micro-Particle Image Velocimetry using phase-correlation and confocal microscopy," *Microfluid. Nanofluid.*, vol. 14, no. 3, pp. 431–444, 2013.
[222] F. Hild, B. Raka, M. Baudequin, S. Roux, and F. Cantelaube, "Multiscale displacement field measurements of compressed mineral-wool samples by digital image correlation," *Appl. Opt.*, vol. 41, no. 32, pp. 6815–6828, 2002.
[223] T. Sawada and M. Sakamoto, "High-resolution large-strain measurement of plastically deformed specimen by Fourier phase correlation," *Int. J. Mech. Sci.*, vol. 49, no. 7, pp. 861–871, 2007.
[224] H. Wang, J. Zhao, J. Zhao, J. Song, Z. Pan, and X. Jiang, "A new rapid-precision position measurement method for a linear motor mover based on a 1-D EPCA," *IEEE Trans. Ind. Electron.*, vol. 65, no. 9, pp. 7485–7494, Sep. 2018.
[225] M. Birem, R. Kleihorst, and N. El-Ghouti, "Visual odometry based on the Fourier transform using a monocular ground-facing camera," *J. Real-Time Image Process.*, vol. 14, no. 3, pp. 637–646, 2018.
[226] X. Tang, J. Xie, X. Wang, and W. Jiang, "High-precision attitude post-processing and initial verification for the ZY-3 satellite," *Remote Sens.*, vol. 7, no. 1, 2015, Art. no. 111.
[227] Z. Ye, Y. Xu, L. Hoegner, X. Tong, and U. Stilla, "Precise disparity estimation for narrow baseline stereo based on multiscale superpixels and phase correlation," in *Proc. Int. Arch. Photogramm., Remote Sens. Spatial Inf. Sci.*, Enschede, The Netherlands, 2019, pp. 147–153.
[228] H. Han, J. Im, and H.-C. Kim, "Variations in ice velocities of Pine Island Glacier Ice Shelf evaluated using multispectral image matching of Landsat time series data," *Remote Sens. Environ.*, vol. 186, pp. 358–371, 2016.
[229] N. Schaffer, L. Copland, and C. Zdanowicz, "Ice velocity changes on Penny Ice Cap, Baffin Island, since the 1950s," *J. Glaciol.*, vol. 63, no. 240, pp. 716–730, 2017.
[230] D. Sakakibara and S. Sugiyama, "Ice front and flow speed variations of marine-terminating outlet glaciers along the coast of Prudhoe Land, northwestern Greenland," *J. Glaciol.*, vol. 64, no. 244, pp. 300–310, 2018.
[231] J.-P. Avouac *et al.*, "The 2013, Mw 7.7 Balochistan earthquake, energetic strike-slip reactivation of a thrust fault," *Earth Planet. Sci. Lett.*, vol. 391, pp. 128–134, 2014.
[232] J. R. Elliott *et al.*, "Himalayan megathrust geometry and relation to topography revealed by the Gorkha earthquake," *Nature Geosci.*, vol. 9, pp. 174–180, 2016.
[233] A. Socquet, J. Hollingsworth, E. Pathier, and M. Bouchon, "Evidence of supershear during the 2018 magnitude 7.5 Palu earthquake from space geodesy," *Nature Geosci.*, vol. 12, no. 3, pp. 192–199, 2019.
[234] P. Gantayat, A. V. Kulkarni, and J. Srinivasan, "Estimation of ice thickness using surface velocities and slope: Case study at Gangotri Glacier, India," *J. Glaciol.*, vol. 60, no. 220, pp. 277–282, 2014.
[235] W. H. Armstrong, R. S. Anderson, J. Allen, and H. Rajaram, "Modeling the WorldView-derived seasonal velocity evolution of Kennicott Glacier, Alaska," *J. Glaciol.*, vol. 62, no. 234, pp. 763–777, 2016.
[236] Q. Shen, H. Wang, C. K. Shum, L. Jiang, H. T. Hsu, and J. Dong, "Recent high-resolution Antarctic ice velocity maps reveal increased mass loss in Wilkes Land, East Antarctica," *Sci. Rep.*, vol. 8, no. 1, 2018, Art. no. 4477.
[237] A. Stumpf, J. P. Malet, P. Allemand, and P. Ulrich, "Surface reconstruction and landslide displacement measurements with Pléiades satellite images," *ISPRS J. Photogramm. Remote Sens.*, vol. 95, pp. 1–12, 2014.
[238] D. Turner, A. Lucieer, and S. de Jong, "Time series analysis of landslide dynamics using an Unmanned Aerial Vehicle (UAV)," *Remote Sens.*, vol. 7, no. 2, pp. 1736–1757, 2015.
[239] N. Bontemps, P. Lacroix, and M.-P. Doin, "Inversion of deformation fields time-series from optical images, and application to the long term kinematics of slow-moving landslides in Peru," *Remote Sens. Environ.*, vol. 210, pp. 144–158, 2018.
[240] F. Ayoub *et al.*, "Threshold for sand mobility on Mars calibrated from seasonal variations of sand flux," *Nature Commun.*, vol. 5, 2014, Art. no. 5096.
[241] S. Michel, J.-P. Avouac, F. Ayoub, R. C. Ewing, N. Vriend, and E. Heggy, "Comparing dune migration measured from remote sensing with sand flux prediction based on weather data and model, a test case in Qatar," *Earth Planet. Sci. Lett.*, vol. 497, pp. 12–21, 2018.
[242] R. Mumtaz and P. Palmer, "Attitude determination by exploiting geometric distortions in stereo images of DMC camera," *IEEE Trans. Aerosp. Electron. Syst.*, vol. 49, no. 3, pp. 1601–1625, Jul. 2013.
[243] X. Tong *et al.*, "Attitude oscillation detection of the ZY-3 satellite by using multispectral parallax images," *IEEE Trans. Geosci. Remote Sens.*, vol. 53, no. 6, pp. 3522–3534, Jun. 2015.
[244] Z. Ye *et al.*, "Estimation of the attitude perturbance using parallax imagery-Application to ZY-3 satellite," in *Proc. ISPRS Ann. Photogram., Remote Sens. Spatial Inform. Sci.*, Munich, Germany, 2015, pp. 279–283.
[245] J. Almonacid-Caballer, J. Pardo-Pascual, and L. Ruiz, "Evaluating Fourier cross-correlation sub-pixel registration in Landsat images," *Remote Sens.*, vol. 9, no. 10, 2017, Art. no. 1051.
[246] S. Skakun, E. Vermote, J. C. Roger, and C. Justice, "Multispectral misregistration of Sentinel-2A images: Analysis and implications for potential applications," *IEEE Geosci. Remote Sens. Lett.*, vol. 14, no. 12, pp. 2408–2412, Dec. 2017.
[247] A.-M. Rosu, M. Pierrot-Deseilligny, A. Delorme, R. Binet, and Y. Klinger, "Measurement of ground displacement from optical satellite image correlation using the free open-source software MicMac," *ISPRS J. Photogramm. Remote Sens.*, vol. 100, pp. 48–59, 2015.
[248] V. Argyriou and T. Vlachos, "Quad-tree motion estimation in the frequency domain using gradient correlation," *IEEE Trans. Multimedia*, vol. 9, no. 6, pp. 1147–1154, Oct. 2007.

Xiaohua Tong (SM'16) received the Ph.D. degree from Tongji University, Shanghai, China, in 1999.

He was a Research Fellow with Hong Kong Polytechnic University, Hong Kong, in 2006, and a Visiting Scholar with the University of California, Santa Barbara, CA, USA, between 2008 and 2009. He is currently a Professor with the College of Surveying and Geoinformatics, Tongji University. His research interests include remote sensing, geographic information system, uncertainty and spatial data quality, and image processing for high-resolution and hyperspectral images.

Zhen Ye received the B.E. and the Ph.D. degrees from Tongji University, Shanghai, China, in 2011 and 2018, respectively.

He is currently a Postdoctoral Researcher with the Chair of Photogrammetry and Remote Sensing, Technische Universität München, Munich, Germany. His research interests include photogrammetry and remote sensing, high-accuracy image registration, and high-resolution satellite image processing.

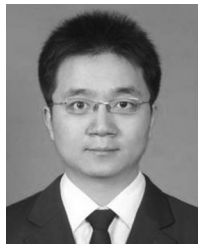

Yusheng Xu (S'17–M'19) was born in 1989. He received the B.S and the M.E degrees from Tongji University, Shanghai, China, in 2011 and 2014, respectively, and the Ph.D. degree (*summa cum laude*) in photogrammetry and remote sensing from Technische Universität München, Munich, Germany, in 2019.

Since 2017, he has been a Scientific Collaborator and Lecturer within the Chair of Photogrammetry and Remote Sensing of Technische Universität München. His research interests include point clouds processing, 3-D reconstruction, image processing, and photogrammetry.

Sa Gao was born in 1991. He received the B.E. degree from Tongji University, Shanghai, China, in 2014. He is currently working toward the Ph.D. degree with the College of Surveying and Geo-informatics, Tongji University.

His research interests include videogrammetry, noncontact deformation measurement, and underwater photogrammetry.

Huan Xie (M'14) received the B.S. degree in surveying engineering, and the M.S. and the Ph.D. degrees in cartography and geoinformation from Tongji University, Shanghai, China, in 2003, 2006, and 2009, respectively.

From 2007 to 2008, she was a Visiting Student with the Institute of Photogrammetry and Geoinformation, Leibniz Universität, Hannover, Germany. She is currently a Professor with the College of Surveying and Geo-Informatics, Tongji University. Her research interests include hyperspectral remote sensing and polar remote sensing.

Qian Du (S'98–M'00–SM'05–F'18) received the Ph.D. degree in electrical engineering from the University of Maryland at Baltimore County, Baltimore, MD, USA, in 2000.

She is currently the Bobby Shackouls Professor with the Department of Electrical and Computer Engineering, Mississippi State University, Starkville, MS, USA. She is also an Adjunct Professor with the College of Surveying and Geo-informatics, Tongji University, Shanghai, China. Her research interests include hyperspectral remote sensing image analysis and applications, pattern classification, data compression, and neural networks.

Dr. Du is a Fellow of the SPIE-International Society for Optics and Photonics. She was the recipient of the 2010 Best Reviewer Award from the IEEE Geoscience and Remote Sensing Society. She was an Associate Editor for the IEEE JOURNAL OF SELECTED TOPICS IN APPLIED EARTH OBSERVATIONS AND REMOTE SENSING, *Journal of Applied Remote Sensing*, and IEEE SIGNAL PROCESSING LETTERS. Since 2016, she has been the Editor-in-Chief for the IEEE JOURNAL OF SELECTED TOPICS IN APPLIED EARTH OBSERVATIONS AND REMOTE SENSING. She was a Co-Chair of the Data Fusion Technical Committee of the IEEE Geoscience and Remote Sensing Society from 2009 to 2013, and the Chair of the Remote Sensing and Mapping Technical Committee of the International Association for Pattern Recognition from 2010 to 2014. She was also the General Chair of the 4th IEEE GRSS Workshop on Hyperspectral Image and Signal Processing: Evolution in Remote Sensing, Shanghai, China, in 2012.

Shijie Liu received the B.S., M.S., and Ph.D. degrees from Tongji University, Shanghai, China, in 2005, 2008, and 2012, respectively.

He is currently an Associate Professor of surveying and mapping science and technology with the College of Surveying and Geoinformatics, Tongji University. His research interests include geometric exploitation of high-resolution remote sensing imagery and its application.

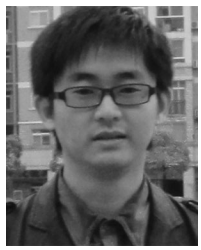

Xiong Xu (M'16) received the B.S. and Ph.D. degrees in photogrammetry from Wuhan University, Wuhan, China, in 2008 and 2013, respectively.

He was a Postdoctoral Researcher with Prof. Antonio Plaza (IEEE Fellow) between 2014 and 2017. He is currently an Associate Professor with the College of Surveying and Geoinformatics, Tongji University, China. His research interests include multispectral and hyperspectral image processing, deep learning in remote sensing, and remote sensing applications.

Sicong Liu (S'13–M'15) received the B.Sc. degree in geographical information system and the M.E. degree in photogrammetry and remote sensing from the China University of Mining and Technology, Xuzhou, China, in 2009 and 2011, respectively, and the Ph.D. degree in information and communication technology from the University of Trento, Trento, Italy, 2015.

He is currently an Assistant Professor with the College of Surveying and Geo-Informatics, Tongji University, Shanghai, China. His research interests include multitemporal remote sensing data analysis, change detection, multispectral/hyperspectral remote sensing, signal processing, and pattern recognition.

Dr. Liu was the winner (ranked at third place) of the Paper Contest of the 2014 IEEE GRSS Data Fusion Contest. He has served as the Session Chair for many international conferences, such as the International Geoscience and Remote Sensing Symposium. He is the Technical Co-Chair of the Tenth International Workshop on the Analysis of Multitemporal Remote Sensing Images (MultiTemp 2019). He is also a Referee for more than 20 international journals.

Kuifeng Luan received the Ph.D. degree from Tongji University, Shanghai, China, in 2018.

He is currently a Lecturer with the College of Marine Sciences, Shanghai Ocean University. His research interests include photogrammetry and remote sensing, Laser 3-D imaging, and single photon LIDAR data processing.

Uwe Stilla (M'04–SM'09) was born in Cologne, Germany, in 1957. He received the Dipl.Ing. degree in electrical engineering from Gesamthochschule Paderborn, Paderborn, Germany, in 1980, and the Dipl.Ing. degree in biomedical engineering and the Ph.D. (Doctor of Engineering) degree in pattern recognition from the University of Karlsruhe, Karlsruhe, Germany, in 1987, and 1993, respectively.

From 1990 to 2004, he was with the Institute of Optronics and Pattern Recognition, Ettlingen, Germany, a German research establishment for defense-related studies. Since 2004, he has been a Professor with the Technical University of Munich (TUM), Munich, Germany, and the Head of the Department of Photogrammetry and Remote Sensing. He was the Vice Dean of the Faculty of Civil, Geo, and Environmental Engineering, and is currently the Dean of Studies of the bachelor's and master's programs Geodesy and Geoinformation, Earth Oriented Space Science and Technology, and Cartography. He has authored/coauthored more than 350 entries. His research interests include image analysis in the field of photogrammetry and remote sensing.

Dr. Stilla is the Chair of the ISPRS Working Group II/III Pattern Analysis in Remote Sensing, a Principal Investigator of the International Graduate School of Science and Engineering, the President of the German Society of Photogrammetry, Remote Sensing and Geoinformation, a member of the Scientific Board of German Commission of Geodesy, and a member of the Commission for Geodesy and Glaciology, Bavarian Academy of Science and Humanities, Munich, Germany.